In Vivo Analysis of the Stability and Transport of Nuclear Poly(A)$^+$ RNA

Sui Huang, Thomas J. Deerinck,* Mark H. Ellisman,* and David L. Spector

Cold Spring Harbor Laboratory, Cold Spring Harbor, New York 11724; and *University of California at San Diego, Department of Neurosciences and San Diego Microscopy and Imaging Resource, La Jolla, California 92093

Abstract. We have studied the distribution of poly(A)$^+$ RNA in the mammalian cell nucleus and its transport through nuclear pores by fluorescence and electron microscopic in situ hybridization. Poly(A)$^+$ RNA was detected in the nucleus as a speckled pattern which includes interchromatin granule clusters and perichromatin fibrils. When cells are fractionated by detergent and salt extraction as well as DNase I digestion, the majority of the nuclear poly(A)$^+$ RNA was found to remain associated with the nonchromatin RNP-enriched fraction of the nucleus. After inhibition of RNA polymerase II transcription for 5–10 h, a stable population of poly(A)$^+$ RNA remained in the nucleus and was reorganized into fewer and larger interchromatin granule clusters along with pre-mRNA splicing factors. This stable population of nuclear RNA may play an important role in nuclear function. Furthermore, we have observed that, in actively transcribing cells, the regions of poly(A)$^+$ RNA which reached the nuclear pore complexes appeared as narrow concentrations of RNA suggesting a limited or directed pathway of movement. All of the observed nuclear pores contained poly(A)$^+$ RNA staining suggesting that they are all capable of exporting RNA. In addition, we have directly visualized, for the first time in mammalian cells, the transport of poly(A)$^+$ RNA through the nuclear pore complexes.

THE majority of pre-mRNAs transcribed by RNA polymerase II undergo a maturation process prior to their transport from the nucleus to the cytoplasm. For most transcripts, the maturation process includes capping at the 5′ end, addition of poly(A) to the 3′ end, and splicing of noncoding regions. The splicing activity involves the formation of spliceosome complexes composed of as many as 50 proteins and snRNAs (Reed, 1990). The role of many of these components are well characterized both in vivo and in vitro (reviewed in Green, 1991; Moore et al., 1993). At the cellular level, the organization of splicing factors has been extensively studied by immunocytochemistry and in situ hybridization. Localization using antibodies specific to snRNP proteins, and non-snRNP splicing factors, such as SC35, have shown that these splicing factors are distributed in a speckled pattern in the interphase nucleus and certain of these factors are also present in coiled bodies (for a review see Spector, 1993). In situ hybridization with oligonucleotides complementary to the major spliceosomal snRNAs resulted in a similar observation (Carmo-Fonseca et al., 1991*a*, 1992; Huang and Spector, 1992).

When examined by electron microscopy, the speckled pattern was found to correspond to both interchromatin granule clusters and perichromatin fibrils (Fakan et al., 1984; Spector et al., 1991). Three-dimensional reconstruction at the fluorescence and electron microscopic levels has shown that some of the interchromatin granule clusters and perichromatin fibrils interconnect (Spector, 1990; Spector et al., 1991). Interchromatin granule clusters do not appear to be labeled after short pulses with [^{3}H]uridine (for a review see Fakan and Puvion, 1980) and exhibit little to no staining with anti-DNA (Turner and Franchi, 1987) or anti-RNA polymerase II (Spector et al., 1993) antibodies. Therefore, it has been suggested that interchromatin granule clusters may represent storage and/or reassembly sites of snRNPs and non-snRNP splicing factors (Jiménez-García and Spector, 1993). Perichromatin fibrils, however, label with [^{3}H]uridine (for a review see Fakan and Puvion, 1980) and anti-RNA polymerase II antibodies (Spector et al., 1993) suggesting that they represent nascent transcripts. The elaborate organization of splicing factors as a speckled pattern has been shown to be functionally related to the transcriptional and splicing activities of the cell (Fakan and Puvion, 1980; Jiménez-García and Spector, 1993; O'Keefe et al., 1994). When cells were infected with adenovirus 2 or were transiently transfected with a rat β-tropomyosin expression vector driven by the SV-40 promoter, splicing factors were recruited to the newly introduced highly active transcription sites. Furthermore, when oligonucleotides or antibodies which inhibit pre-mRNA splicing in vitro were introduced into cells, splicing factors reorganized to large interchromatin granule clusters

Address all correspondence to D. L. Spector, Cold Spring Harbor Laboratory, One Bungtown Road, Cold Spring Harbor, NY 11724.

(O'Keefe et al., 1994). These results suggested that the nuclear organization of splicing factors is dynamic and that these factors shuttle between storage and/or reassembly sites (interchromatin granule clusters) and sites of active transcription and pre-mRNA splicing (Jiménez-García and Spector, 1993; O'Keefe et al., 1994).

If the speckled pattern is a reflection of RNA polymerase II transcription, one would expect that nascent RNA transcripts are closely associated with these nuclear regions. Recently, RNA transcripts from two endogenous genes, c-fos and fibronectin, were shown to be spatially associated with the periphery of a subset of nuclear speckles (Huang and Spector, 1991; Xing et al., 1993). Thiry (1993) has used in situ polyadenylate nucleotidyl transferase or anti-RNA antibodies to label RNA on cell sections and has found labeling over interchromatin granule clusters. However, the species of RNA labeled were not determined. Poly(A)$^+$ RNA has been previously localized to the entire speckled pattern by fluorescence in situ hybridization (Carter et al., 1991, 1993). Based upon this localization, the authors (Carter et al., 1991, 1993) refer to the speckled regions as transcript domains and suggest that these regions may represent active transcription sites. The localization of poly(A)$^+$ RNA to the entire speckled pattern was surprising in light of the fact that part of the speckled pattern, interchromatin granule clusters, did not label after pulses, from 2 min up to several hours, with [^{3}H]uridine (for a review see Fakan and Puvion, 1980) or short pulses with bromo-UTP (Jackson et al., 1993; Wansink et al., 1993), and little to no DNA or RNA polymerase II is found in these clusters (for a review see Spector, 1993). However, labeling with [^{3}H]uridine for 6 h followed by a chase of 24 h resulted in a higher frequency of labeling of interchromatin granule clusters (Fakan and Bernhard, 1973). There are at least two possible explanations for these observed differences. First, since perichromatin fibrils are to some extent located on the periphery of interchromatin granule clusters, the staining of the periphery of the clusters with a strong fluorescent probe could result in fluorescent flare that exceeds the resolution of the light microscope resulting in an image which appears to stain the entire cluster when in fact it is only staining the periphery of the cluster. A high-resolution electron microscopic analysis attempted to address this possibility (Visa et al., 1993). However, due to the low level of labeling, the amount of poly(A)$^+$ RNA in interchromatin granule clusters is unclear. A second possibility is that there is a stable population of poly(A)$^+$ RNA localized to the interchromatin granule clusters which does not translocate into the cytoplasm. To distinguish between these two possibilities, and to examine the organization of poly(A)$^+$ RNA at higher resolution, we have localized poly(A)$^+$ RNA using two different electron microscopic approaches in both actively transcribing cells and in cells where RNA polymerase II has been inactivated. Both methods demonstrated poly(A)$^+$ RNA to be localized to interchromatin granule clusters as well as perichromatin fibrils. When transcription by RNA polymerase II was inhibited, a large amount of poly(A)$^+$ RNA remained in the nucleus and was associated with fused interchromatin granule clusters. These observations suggest that the population of stable poly(A)$^+$ RNA, which is associated with the interchromatin granule clusters, may serve functional roles in the cell nucleus other than being pre-mRNA or mRNA. In addition, in actively transcribing cells, a narrow bridgelike staining was observed connecting the intranuclear RNA clusters to the nuclear pore complexes suggesting that RNA transport is a directed process. We have also directly visualized poly(A)$^+$ RNA in the process of being transported through the nuclear pores.

Materials and Methods

Cell Culture and Transcription Inhibition

HeLa cells and Wacar, primary human skin fibroblast cells, were grown in DME. CHO cells were grown in F12 medium and Amal cells (α-amanitin resistant derivative of CHO cells) were grown in MEM. All media were supplemented with 10% fetal calf serum (GIBCO BRL, Gaithersburg, MD) and cells were maintained at 37°C with 10% CO_2. Cells were grown on glass coverslips in 35-mm-diam Petri dishes. For photooxidation experiments cells were grown on special tissue culture dishes (Mattek Corp., Ashland, MA) incorporating a coverslip on the bottom to facilitate visualization with an inverted microscope.

The experiments presented in this paper have been repeated an average of 10 times. The localization patterns presented were observed in all of the cells examined. Thousands of cells were examined at the fluorescence microscopic level and dozens of cells were examined at the electron microscopic level.

RNA polymerase II inhibition was achieved by the addition of α-amanitin (5–50 μg/ml for 5-10 h) or 5,6-dichloro-1-β-D-ribofuranosylbenzimidazole (DRB)[1] (25 μg/ml for 3 h) to the culture medium. For DRB reversal, the medium containing the drug was removed, cells were washed with drug-free medium three times and cells were allowed to recover by incubation in drug-free medium for 2 h. RNA polymerase III inhibition was achieved by the addition of α-amanitin (250 μg/ml) for 5–10 h.

Nuclear Fractionation

Nuclear fractionation was carried out according to the procedure described by Fey et al. (1986). Cells were washed with cold PBS and incubated at 4°C for 10 min in cytoskeleton (CSK) buffer (100 mM NaCl, 300 mM sucrose, 10 mM Pipes, pH 6.8, 3 mM $MgCl_2$, 10 μM leupeptin, 2 mM vanadyl adenosine, and 0.5% Triton X-100). Cells were then incubated at 4°C for 5 min in extraction buffer (250 mM ammonium sulfate, 300 mM sucrose, 10 mM Pipes, pH 6.8, 3 mM $MgCl_2$, 10 μM leupeptin, 2 mM vanadyl adenosine, and 0.5% Triton X-100). Cells were then treated with 100 μg/ml DNAse I in CSK buffer with 50 mM NaCl for 40 min to remove chromatin. The DNAse I activity was terminated in CSK buffer containing 250 mM ammonium sulphate.

In Situ Hybridization

Cells at subconfluence were prepared for fluorescence in situ hybridization by rinsing with PBS and fixing in 4% formaldehyde for 15 min at room temperature. For electron microscopic examination, cells were fixed in 4% formaldehyde and 0.01–0.05% glutaraldehyde for 15 min at room temperature. Cells were then washed 3 × 15 min, in PBS or PBS plus 0.3 M glycine in the case of glutaraldehyde fixation, and permeabilized with 0.5% Triton X-100 for 5 min at 4°C. Cells were again rinsed in PBS 2 × 15 min. An oligo dT 50 mer ($dT_{[50]}$) was 3' end labeled with either biotin, FITC (Operon Technols Inc., Alameda, CA), or digoxigenin (Genius labeling kit; Boehringer Mannheim Biochemicals, Indianapolis, IN), and was used as a probe for in situ hybridization to poly(A)$^+$ RNA. Cells were equilibrated in 2× SSC for 10 min and were then subjected to hybridization. The hybridization mixture (20 μl) contained 80 ng Oligo $dT_{(50)}$, 2× SSC, 1 mg/ml of tRNA, 10% dextran sulfate, and 25% formamide. Hybridization was performed at 42°C in a humidified chamber overnight. After hybridization, cells were washed 2 × 15 min each, in 2× SSC, and 15 min in 0.5× SSC.

DNAse I and RNAse Digestions

DNAse I, RNAse A, and T2 digestions were carried out after cells were permeabilized by 0.5% Triton X-100. Cells were washed 3 × 10 min and

1. *Abbreviations used in this paper*: CSK, cytoskeleton; DRB, 5,6-dichloro-1-β-D-ribofuranosylbenzimidazole; NGS, normal goat serum; NuMA, nuclear-mitotic apparatus protein.

incubated with 100 U/ml DNAse I in PBS plus 5 mM $MgCl_2$, or 200 μg/ml RNAse A, or with 100 U/ml RNAse T2 in PBS for 2 h at 37°C. Cells were then washed in PBS and subjected to hybridization. RNAse H digestion was carried out after hybridization with the specific probe. Cells were washed with 2× SSC and 0.5× SSC posthybridization as described above. Cells were then equilibrated with the RNAse H digestion buffer (20 mM Hepes-KOH, pH 8.0, 50 mM KCl, 10 mM $MgCl_2$, 1 mM dithiothreitol) for 10 min and incubated with 0.1 U RNase H/μl in the same buffer for 2 h at 37°C. Cells were washed with 2× SSC for 2 × 15 min and 0.5× SSC for 15 min before mounting.

Immunolabeling

After hybridization, cells were washed 3 × 10 min in PBS and incubated with anti-SC35 primary antibody ascites (Fu and Maniatis, 1990) at a dilution of 1:1,000 for 1 h at room temperature. Cells were rinsed in PBS and then incubated with Texas red–conjugated goat anti–mouse antibody at a dilution of 1:30 for 1 h at room temperature, followed by three washes in PBS.

Signal Detection by Fluorescence Microscopy

Hybridizations with biotinylated oligonucleotides were detected by FITC-conjugated avidin (Vector Labs, Inc., Burlingame, CA) at 2 μg/ml as described by Huang and Spector (1992). Hybridizations with the digoxigenin-labeled probe were detected with FITC-conjugated anti–digoxigenin Fab′ (Boehringer Mannheim Biochemicals) at a dilution of 1:20–1:40. Cells were incubated in antibody for 1 h at room temperature. Cells were then washed with PBS or PBS plus 0.1% Triton X-100. The coverslips were mounted onto glass slides with mounting medium containing 90% glycerol in 0.2M Tris-base (pH 8.0) with 1 mg/ml paraphenylenediamine as an antifading agent. Cells were examined with a Nikon FXA microscope equipped with epifluorescence and differential interference contrast optics.

Pre-embedding Gold In Situ Hybridization

Following hybridization with the digoxigenin-labeled oligo $dT_{(50)}$ as described above, cells were probed by monoclonal anti–digoxin antibody (Sigma Chemicals Co., St. Louis, MO) with 1% normal goat serum (NGS) for 1 h at room temperature. The excess antibodies were removed by extensively washing in PBS containing 1% NGS for 5 × 10 min each. Cells were then incubated with goat anti–mouse Fab′ conjugated with FITC and 1.4-nm gold (Nanoprobes Inc., Stony Brook, NY) for 1 h at room temperature followed by extensive washing with PBS. The labeling was monitored by fluorescence microscopy. Cells were subsequently fixed in 1% glutaraldehyde for 15 min and rinsed in several changes of distilled water for 5-min each. Silver enhancement of the 1.4-nm gold was carried out using a silver enhancement kit from Nanoprobes Inc. The enhancement of both experimental and control coverslips was developed under identical conditions. Cells were dehydrated in increasing concentrations of ethanol (70, 80, 90, 95, 100%) and embedded in Epon/Araldite (PolySciences Inc., Warrington, PA) at 60°C overnight. Sections of 100 nm in thickness were cut on a Reichert Ultracut E ultramicrotome and poststained by the EDTA-regressive method (Bernhard, 1969) and examined in a Hitachi H-7000 transmission electron microscope operated at 75 kV.

Photooxidation

After in situ hybridization with biotinylated oligo $dT_{(50)}$, cells were washed 2 × 2 min in 0.1 M PBS, and then incubated in 0.1 M PBS with 1% NGS, 1% cold water fish gelatin, and 1% BSA (fraction V) for 20 min to block nonspecific staining. Cells were then incubated with ~50 μg/ml streptavidin eosin-5-isothiocyanate (conjugated as previously described; Deerinck et al., 1994) diluted in 0.1 M PBS with 1% BSA and 1% NGS for 1 h. Unbound conjugate was removed by washing 6 × 5 min in 0.1 M PBS with 1% BSA and 1% NGS. After 2 × 5 min washes with 0.1 M sodium cacodylate, pH 7.4, cells were washed for 1 min in the same buffer containing 10 μM free biotin to enhance fluorescence. All washes and incubations were at 4°C.

Cells were examined using a Zeiss Axiovert 35M equipped with a MRC-600 laser scanning confocal system (Bio-Rad Labs, Cambridge, MA) using the 488-nm excitation from an argon/krypton laser. During imaging the cells were kept at 10°C using a cold stage and were in 0.1 M sodium cacodylate that had been deoxygenated by bubbling with argon to retard photobleaching.

Once an area had been selected using a 40× 1.3 NA Zeiss planapo objective, a cold oxygenated solution of 1 mg/ml diaminobenzidine tetrahydrochloride (Sigma Chemical Co.) in 0.1 M sodium cacodylate, pH 7.2, was added to the cells. Photooxidation of the DAB by eosin was accomplished by illuminating the region of interest with 515-nm light from either a 200 W mercury or a 75 W xenon source. The progress of the reaction was monitored by transmitted light and illumination was halted when a brownish reaction product became visible (10–20 min). Both experimental and control preparations were reacted under identical conditions.

Following photooxidation, the cells were rinsed 5 × 2 min in 0.1 M sodium cacodylate, and then postfixed in 1% osmium tetroxide for 1 h. Cells were then rinsed in double-distilled water, dehydrated in an ethanol series, and then infiltrated with Durcopan ACM resin (Electron Microscopy Sciences Inc., Fort Washington, PA). Following polymerization of the resin for 24 h at 60°C, the bottom glass coverslip was removed from the dish and the region of interest was cut out and mounted for ultramicrotomy with an Ultracut E (Leica) ultramicrotome using a diamond knife (Diatome). Electron micrographs were recorded from sections 80 nm in thickness at 60–80 kV with a JEOL 100CX and sections of 500–1,000-nm thick at 300–400 kV with a JEOL 4000EX. Stereo-pair images were recorded by tilting the specimen stage to ± 8°. Sections of photooxidized cells were not poststained.

In Situ Autoradiography

Cells were incubated with [^{3}H]uridine (50 μCi/ml) (Amersham Corp., Arlington Heights, IL) in culture medium for 15 min at 37°C. Cells were washed with medium containing 1 mg/ml of uridine, 2 × 5 min each. After fixation in 2% formaldehyde in PBS (pH 7.3) and several subsequent washes with PBS, a monolayer of Ilford K5D emulsion was applied to each coverslip and allowed to dry for 1 h in the dark. Coverslips were stored at 4°C and developed after 11 d of exposure. Development was for 7 min in a solution consisting of 7.5 g Metol, 5.0 g anhydrous sodium sulfite, 2.0 g potassium thiocyanate per 1,000 ml distilled water. Coverslips were then washed in distilled water for 1 min and fixed for 5 min in Kodak fixer. After washing in several changes of distilled water for 30 min, coverslips were mounted, and examined with a 60×/1.4 NA objective using a Nikon FXA microscope.

Results

Mammalian Nuclear Poly(A)$^+$ RNA Is Associated with the Nuclear Matrix

We have used an oligo $dT_{(50)}$ end labeled with biotin, digoxigenin, or FITC as probes to hybridize in situ to the poly(A)$^+$ RNA in mammalian cells. In the nucleus, poly(A)$^+$ RNA appeared to be mostly concentrated in a speckled pattern in addition to being diffusely distributed throughout the nucleoplasm (Fig. 1, *A* and *D*). Cytoplasmic staining was also observed which predominantly accounted for the poly(A)$^+$ RNA serving as messenger RNA being translated in the cytoplasm. The observed nuclear hybridization pattern was similar to what has been previously described by Carter et al. (1991, 1993). Hybridization was performed under high stringency conditions for oligonucleotides (42°C in 25% formamide) and posthybridization washes were made in 0.5× SSC to be sure that the hybridization signal was specific for poly(A)$^+$ tails which have an average length of 200 nucleotides. When cells were pretreated with RNase A or T2 (Fig. 1 *C*), or incubated in hybridization buffer without labeled oligo $dT_{(50)}$ (data not shown), the speckled hybridization signal was not observed. In addition, cells digested with RNase H after hybridization, which digested the RNA of the RNA–DNA duplex, showed a significant decrease in hybridization signal (Fig. 1 *F*). The sensitivity of the hybridization signal to these nuclease digestions suggests that the speckled pattern labeled with oligo $dT_{(50)}$ is the result of hybridization to poly(A)$^+$ RNA instead of cross reactivity with other components. Since transcription varies between transformed and "normal" cells we were interested in determining if there was a difference in the distribution of poly(A)$^+$ RNA in

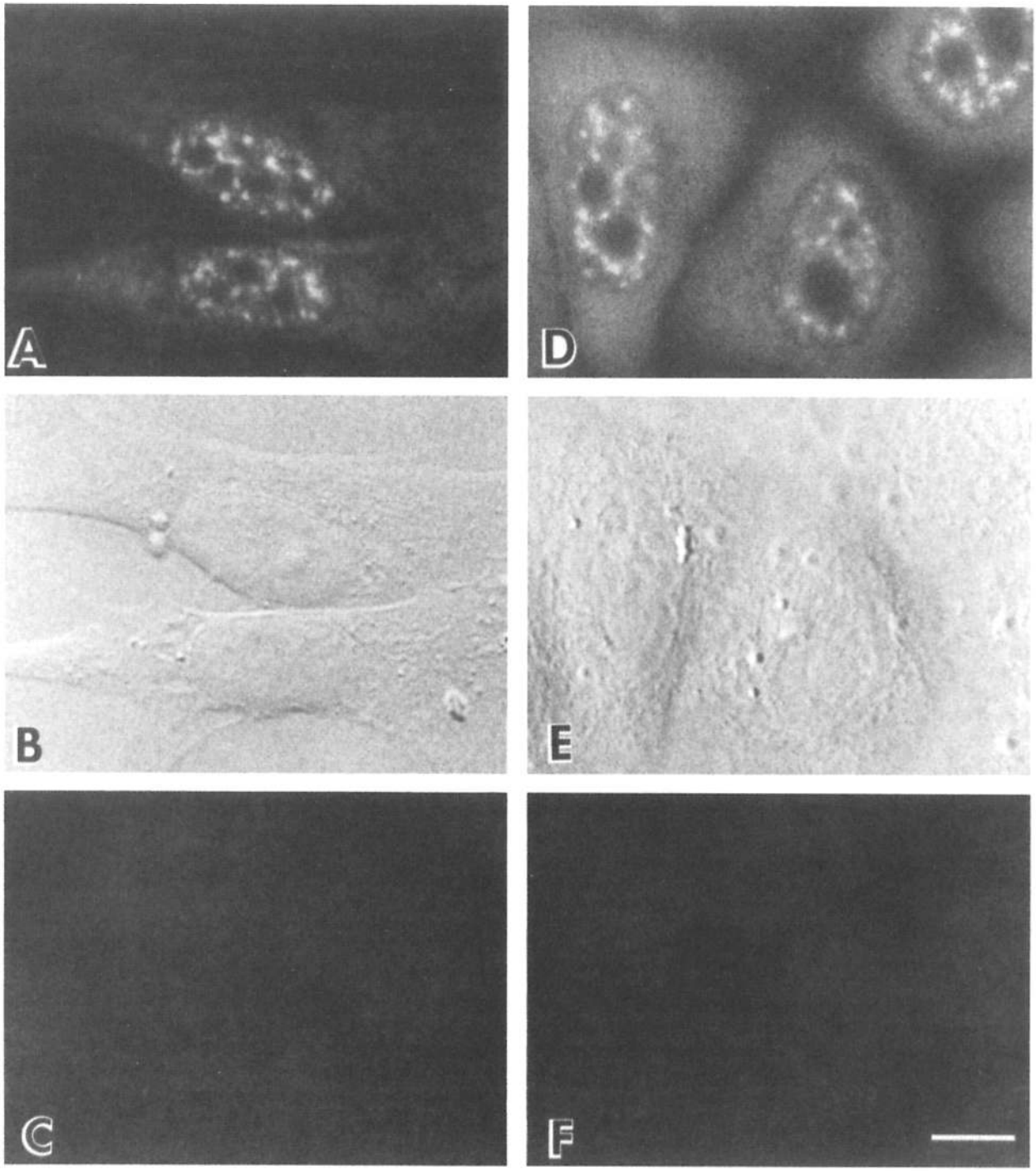

Figure 1. Poly(A)$^+$ RNA distribution is similar in transformed and primary cells. Wacar, human primary fibroblasts (*A*) and HeLa cells (*D*) were in situ hybridized with an oligo $dT_{(50)}$. Poly(A)$^+$ RNA is localized in a speckled nuclear pattern as well as being diffusely distributed in the nucleoplasm and cytoplasm. Cells pretreated with RNase T2 prior to hybridization (*C*) or RNase H posthybridization (*F*) showed no hybridization signal. *B* and *E* are differential interference contrast images of the cells in *A* and *D*. Bar, 10 μm.

these cell types. A direct comparison of Wacar cells (primary human fibroblast cells) (Fig. 1 *A*) with HeLa cells (an epithelial carcinoma cell line) (Fig. 1 *D*) did not reveal a significant difference in the nuclear localization of poly(A)$^+$ RNA.

When nuclei are extracted with nonionic detergents, high salt, and DNAse I, an insoluble fraction remains which has been given the operational definition nuclear matrix (Berezney and Coffey, 1974). When such residual structures are examined in the electron microscope, in addition to the nuclear lamina and a residual nucleolus, an elaborate RNP network is observed (Fey et al., 1986; Smith et al., 1986; He et al., 1990). The integrity of the RNP network is dependent upon the preservation of nuclear RNA (Bouvier et al., 1985; Smith et al., 1986; Berezney, 1991). We were interested in determining if poly(A)$^+$ RNA is associated with this fraction of the nucleus since such an association would help in

our understanding of potential mechanisms of RNA metabolism in the nucleus and RNA transport through the nucleoplasm. We have prepared nuclear matrix from HeLa cells as described previously (Fey et al., 1986). When compared to unextracted cells, the basic speckled pattern of poly(A)$^+$ RNA remained unchanged, however, decreased diffuse nuclear and cytoplasmic staining was observed (Fig. 2 *C*). This result suggests that a large portion of the nuclear poly(A)$^+$ RNA is associated with the insoluble nonchromatin fraction of the nucleus.

Localization of Poly(A)$^+$ RNA by Electron Microscopy

To examine the precise nuclear organization of poly(A)$^+$ RNA and to determine if the speckled pattern observed by fluorescence in situ hybridization represented both interchromatin granule clusters and perichromatin fibrils, the distribution of poly(A)$^+$ RNA was visualized at the electron microscopic level. There are two main approaches to in situ hybridization at the electron microscopic level. One is postembedding in situ hybridization where cells are fixed and embedded in plastic prior to hybridization on sections. Using this method, hybridization will mainly reveal sequences which are at or very close to the surface of the section. An inherent problem with this method is the low level of detectable labeling because of the limited accessibility to complementary sequences for hybridization. A second approach is pre-embedding in situ hybridization where cells are hybridized to a specific probe prior to being embedded in plastic, and therefore, all available sequences are accessible to the probe. Using this second approach, a more quantitative labeling intensity is obtained. Here we describe two different pre-embedding in situ hybridization approaches to localize poly(A)$^+$ RNA at the electron microscopic level.

In the first approach, an oligo $dT_{(50)}$ end labeled with digoxigenin was used to hybridize to poly(A)$^+$ RNA in situ. After hybridization, cells were incubated with mouse monoclonal antibody against digoxin, followed by incubation with goat anti-mouse IgG Fab′ fragments which were covalently conjugated with 1.4-nm gold particles and FITC. The gold particles were then enlarged by silver enhancement to a desirable range for electron microscopic examination. Embedded cells were sectioned and poststained by the EDTA-regressive method (Bernhard, 1969) so that RNP-enriched structures were preferentially revealed. In the nuclei, poly(A)$^+$ RNA was found to be localized to both inter-

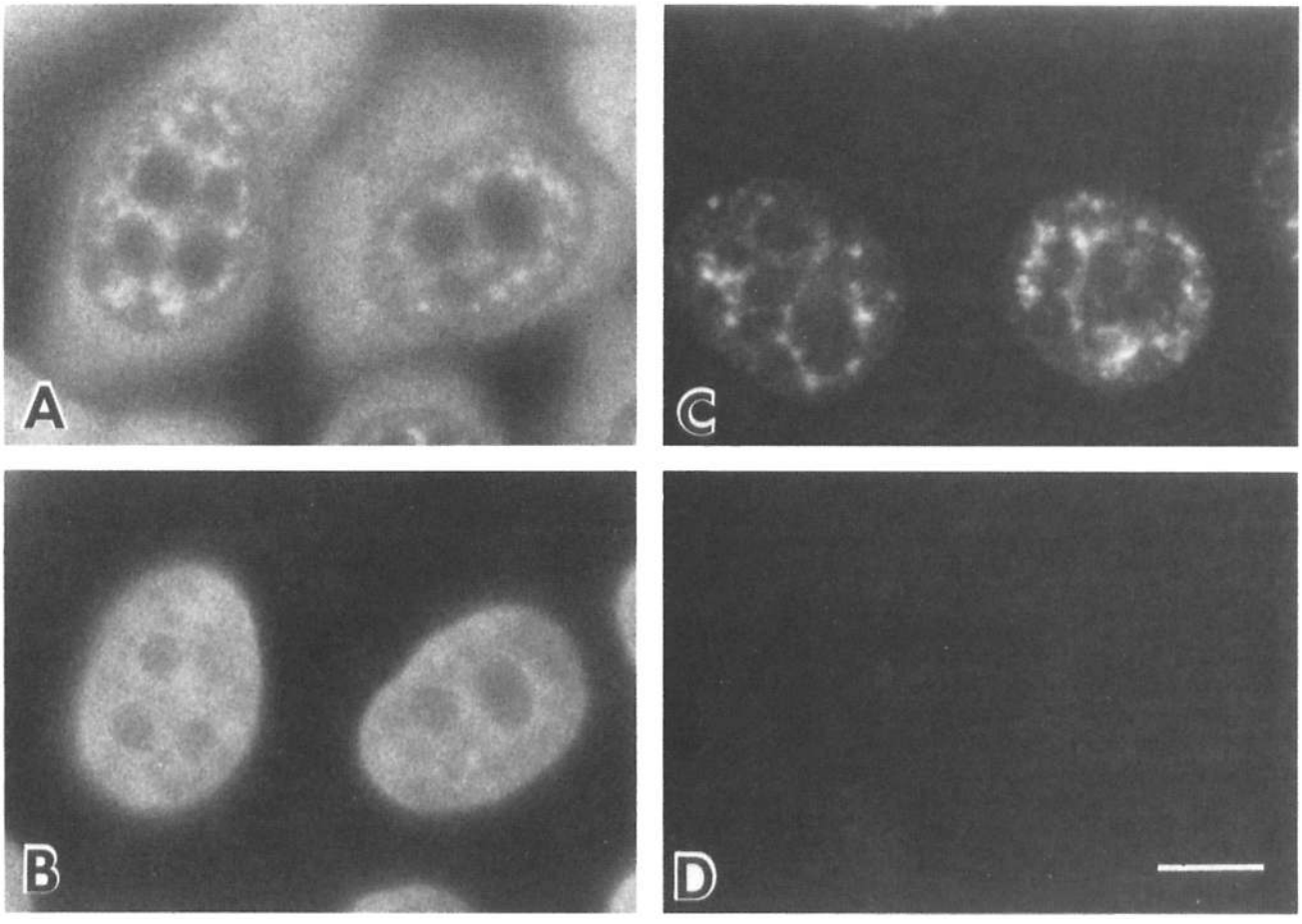

Figure 2. A large portion of poly(A)$^+$ RNA is associated with the nuclear matrix. Poly(A)$^+$ RNA was localized by fluorescence in situ hybridization in whole cells (*A*) and in cells which were extracted with detergent, high salt, and digested with DNAse I (*C*). In unextracted cells poly(A)$^+$ RNA is localized in a speckled nuclear distribution as well as being diffusely distributed in the nucleoplasm and the cytoplasm (*A*). The speckled distribution of poly(A)$^+$ RNA is maintained in nuclear matrix preparations (*C*), however, the diffuse nuclear and cytoplasmic labeling is lost. Cells were probed with an FITC-labeled oligo $dT_{(50)}$ to detect the localization of poly(A)$^+$ RNA (*A* and *C*) and counterstained with Dapi to show the distribution of DNA (*B* and *D*). Bar, 10 μm.

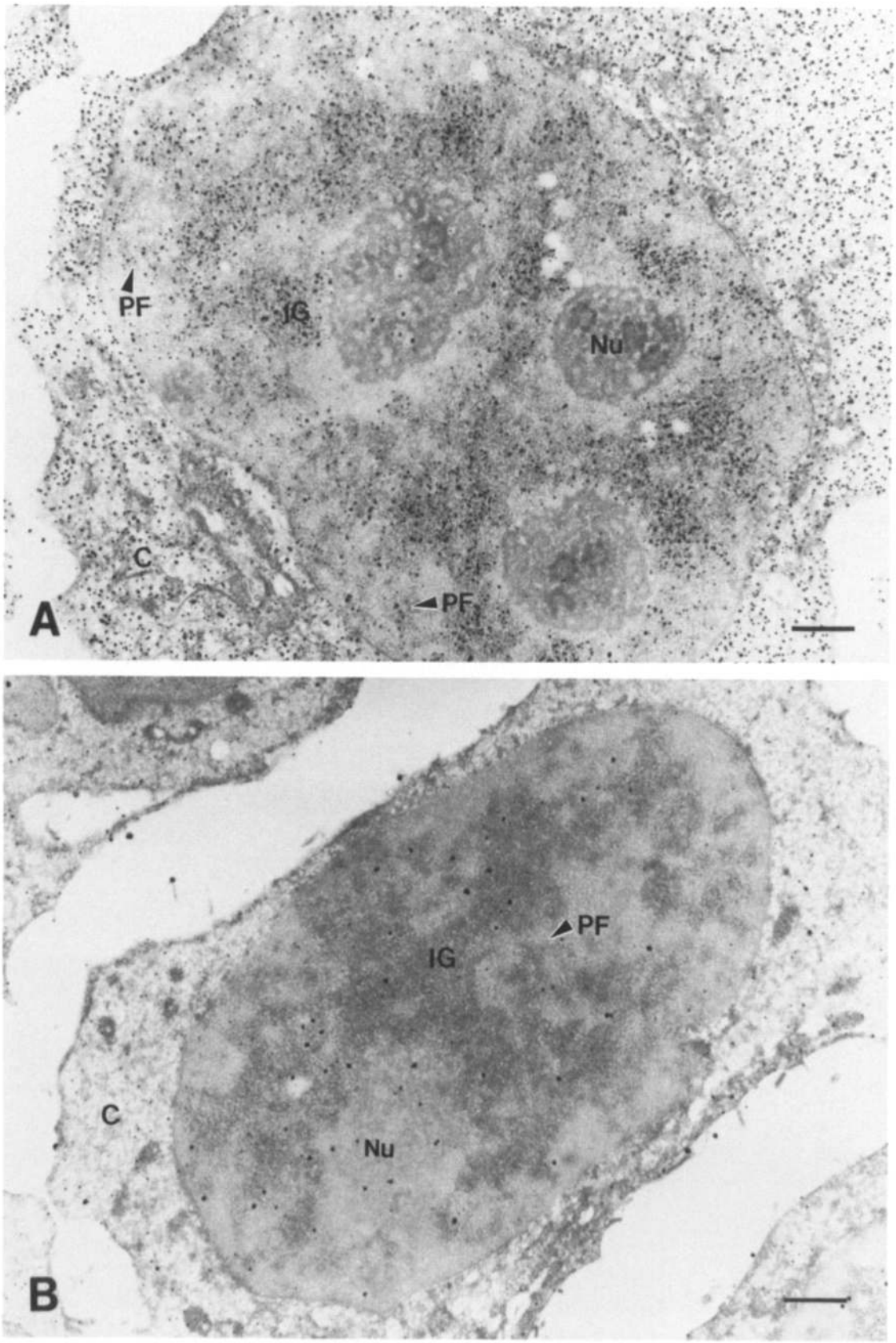

Figure 3. Nuclear poly(A)$^+$ RNA is localized to interchromatin granule clusters (*IG*) and perichromatin fibrils (*PF*) which corresponds to the speckled pattern observed by fluorescence microscopy. Poly(A)$^+$ RNA distribution was examined in HeLa cells by pre-embedding gold labeling EM as described in Materials and Methods. Cells were hybridized with an oligo $dT_{(50)}$ end labeled with digoxigenin and detected by gold-conjugated antibodies (*A*). Cells hybridized in buffer lacking probe showed no hybridization signal (*B*). Cells in both panels were processed simultaneously and were poststained using the EDTA regressive method (Bernhard, 1969) which preferentially stains RNP-enriched structures. Bar, 1 μm.

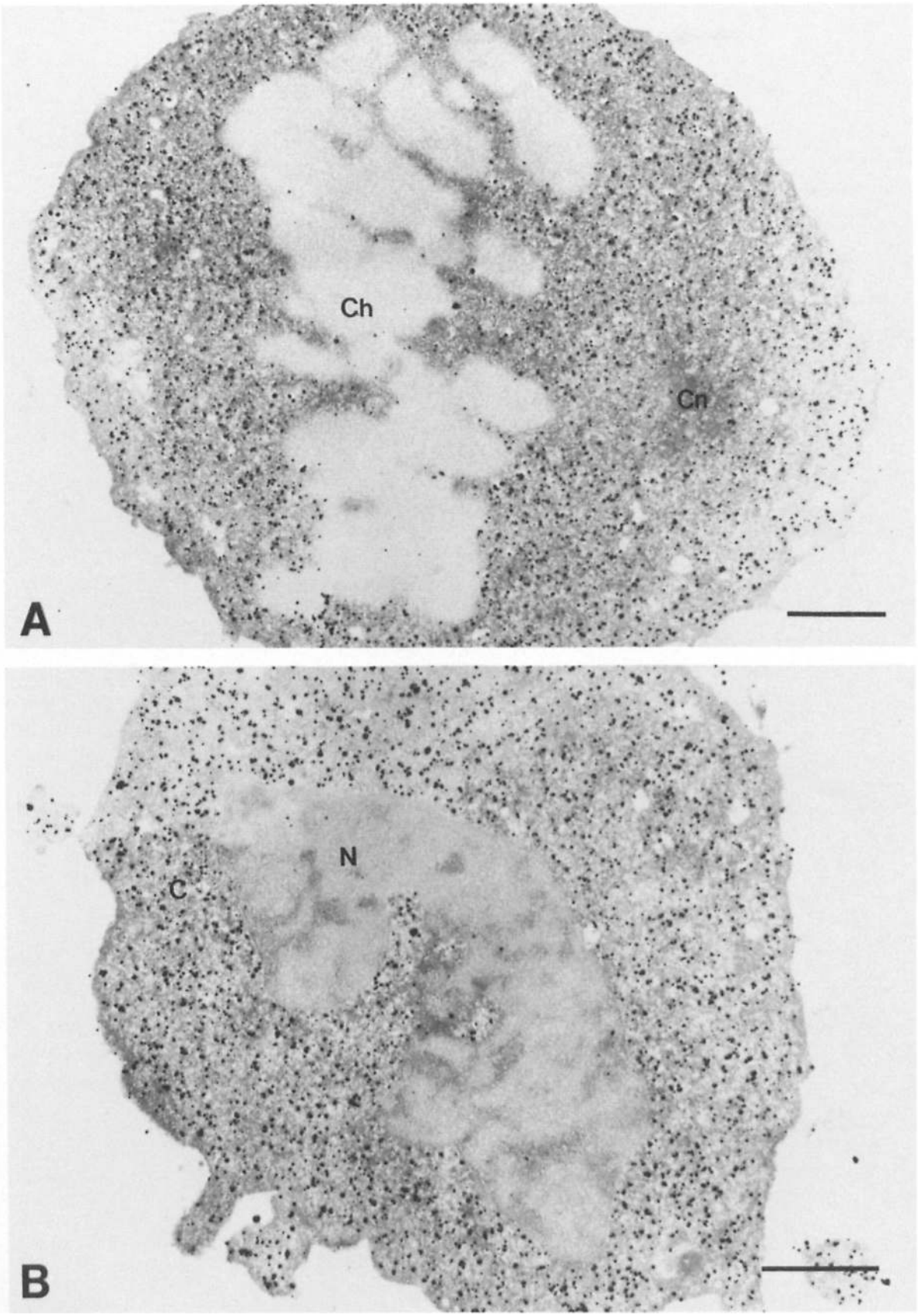

Figure 4. Poly(A)$^+$ RNA organization in cells at different stages of mitosis. In metaphase, poly(A)$^+$ RNA is diffusely distributed throughout the cytoplasm (*A*). The chromosomes (*Ch*) and the centrosome (*Cn*) are not labeled (*A*). In late telophase parental poly(A)$^+$ RNA is excluded from the newly formed nucleus (*B*). Bar, 1 μm.

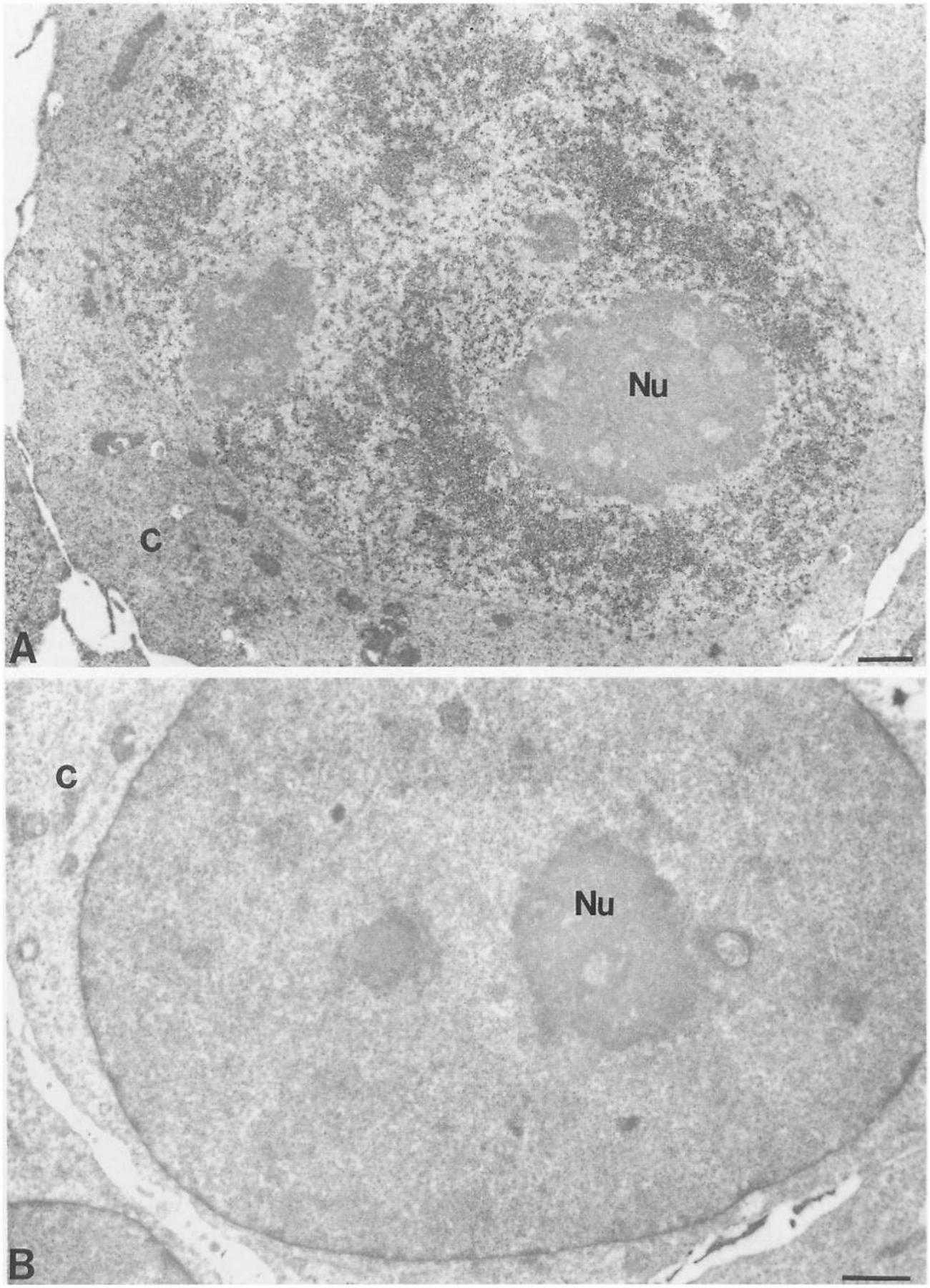

chromatin granule clusters and perichromatin fibrils (Fig. 3 *A*). In fact, poly(A)$^+$ RNA was found to be enriched in interchromatin granule clusters in agreement with the previous fluorescent microscopic studies (Carter et al., 1991, 1993). Sites of Poly(A)$^+$ RNA hybridization extended to the nuclear envelope in several locations (Fig. 3 *A*). The lack of staining in nucleoli, heterochromatin, and in cells hybridized with mock solution without the oligo dT probe (Fig. 3 *B*) demonstrates the specificity of the hybridization signal.

Cells were also examined at different stages of mitosis. During metaphase (Fig. 4 *A*) poly(A)$^+$ RNA can be seen throughout the cytoplasm. However, the chromosomes and the centrosome region are not labeled, further demonstrating the specificity of the hybridization signal. Interestingly, at late telophase when the daughter cell nuclei begin to form, the parental poly(A)$^+$ RNA was excluded from the newly formed nuclei (Fig. 4 *B*). There are two possible explanations for this exclusion. One is that the majority of poly(A)$^+$ RNA is bound to the cytoskeleton so that it is not free to be included in the newly formed nuclei. Alternatively, the formation of the nuclear envelope may selectively include or exclude specific cytoplasmic components.

A second pre-embedding approach to localize poly(A)$^+$ RNA involved using the process of fluorescence photooxidation of DAB by eosin (Deerinck et al., 1994). Using streptavidin-conjugated eosin to detect the hybridized oligo dT labeled with biotin, high-resolution confocal fluorescent images of the distribution of poly(A)$^+$ RNA were obtained. The fluorescent eosin was then used to photooxidize DAB into a stable reaction product that was made electron dense upon exposure to osmium tetroxide. This process allows for high resolution electron microscopic analysis of the distribution of poly(A)$^+$ RNA in mammalian cell nuclei (Fig. 5 *A*). The lack of poly(A)$^+$ RNA labeling in the nucleolar and heterochromatin regions (Fig. 5 *A*) as well as in cells hybridized in mock solution without labeled oligo dT (Fig. 5 *B*) suggests that the hybridization signal observed was specific. Furthermore, the pretreatment with DNAse I prior to the hybridization did not affect the hybridization signal (Fig. 6, *A* and *B*), but the pretreatment with RNAse T2 abolished the poly(A)$^+$ RNA staining completely (Fig. 6, *C* and *D*). Together with the fact that specific hybridization signal was not observed when cells were probed with oligo $dA_{(50)}$ (Fig. 7, *A* and *B*) these controls support the specificity of the hybridization signal observed with the oligo $dT_{(50)}$ probe. We find the photooxidation method to be more sensitive than gold labeling, probably due to accessibility of the secondary detection system. Furthermore, this approach seems to result in less extraction than the pre-embedding gold and silver enhancement methods.

In addition to observing the speckled nuclear distribution of poly(A)$^+$ RNA (Fig. 5 *A*), we have directly visualized the localization of poly(A)$^+$ RNA as it approaches and moves through the nuclear pores (Fig. 8, *A* and *B*). Areas of high concentration of nuclear poly(A)$^+$ RNA appear to taper as they approach nuclear pore complexes (Fig. 8, *A* and *B*). Furthermore, poly(A)$^+$ RNA appears to accumulate on the cytoplasmic side of the nuclear pore complexes (Fig. 8, *A* and *B*). In stereo pairs of 0.5-μm-thick section (Fig. 8 *B*), we have observed extended poly(A)$^+$ RNA labeling exiting the nuclear pore complex into the cytoplasm. When examined in cross section, all of the nuclear pores observed in the section labeled with the oligo $dT_{(50)}$ probe suggesting that all nuclear pores are capable of exporting poly(A)$^+$ RNA to the cytoplasm (Fig. 9 *A*). A close examination of the nuclear pores in cross section shows that the center of the pore complex is less intensely stained than the periphery of the complex (Fig. 9 *B*).

A Population of Stable Poly(A)$^+$ RNA Concentrates in Interchromatin Granule Clusters

The localization of poly(A)$^+$ RNA at the electron microscopic level reveals that poly(A)$^+$ RNA is present within interchromatin granule clusters. As discussed earlier, it is unlikely that the majority of poly(A)$^+$ RNA within these nuclear regions represents newly synthesized RNA because little to no DNA, RNA polymerase II, or [^{3}H]uridine incorporation are present in these regions (for a review see Spector, 1993). Therefore, it is likely that a stable population of poly(A)$^+$ RNA is present in the interchromatin granule clusters. To test this possibility, we have examined the localization of poly(A)$^+$ RNA in the nucleus several hours following inhibition of RNA polymerase II transcription.

The RNA polymerases from mammalian cells can be differentiated from each other on the basis of their sensitivity towards α-amanitin (Stirpe and Fiume, 1967). α-amanitin inhibits transcription by binding stoichiometrically to RNA polymerases forming a tight complex (Jacob et al., 1970; Kedinger et al., 1970; Lindell et al., 1970). CHO cells and Ama 1 cells (Fig. 10) were incubated with α-amanitin at a concentration of 5 μg/ml which specifically inhibits RNA polymerase II, whereas HeLa cells were incubated in α-amanitin at a concentration of 50 μg/ml (data not shown). RNA polymerase I is unaffected by this drug and RNA polymerase III is only affected by higher concentrations of drug, ~250 μg/ml (Weinmann and Roeder, 1974). CHO cells incubated in α-amanitin for 5 h or up to 24 h showed a significant decrease in the level of RNA polymerase II transcription as seen by a dramatic decrease in the number of nucleoplasmic autoradiographic grains in [^{3}H]uridine-labeled cells (Fig. 10, *C* and *D*). RNA polymerase I transcription, however, was not inhibited as there were autoradiographic grains present over the nucleoli (Fig. 10, *C* and *D*). When CHO cells treated with α-amanitin (5–50 μg/ml) for 5 h were analyzed for poly(A)$^+$ RNA labeling, a large amount of poly(A)$^+$ RNA was found to remain in the nuclei (Fig. 11 *B*). Interestingly, the distribution of these RNAs changed into more concen-

Figure 5. Localization of poly(A)$^+$ RNA by pre-embedding in situ hybridization and photooxidation (as described in Materials and Methods) also showed poly(A)$^+$ RNA to localize in a speckled nuclear pattern as well as being diffusely distributed in the nucleoplasm and the cytoplasm (*A*). However, with the increased resolution of this method specific labeling of the nuclear pores was observed. Control cells hybridized without biotinylated probe and which have been processed simultaneously under identical conditions do not show any hybridization signal in the nucleoplasm or the cytoplasm (*B*). Sections were not poststained. Bar, 1 μm.

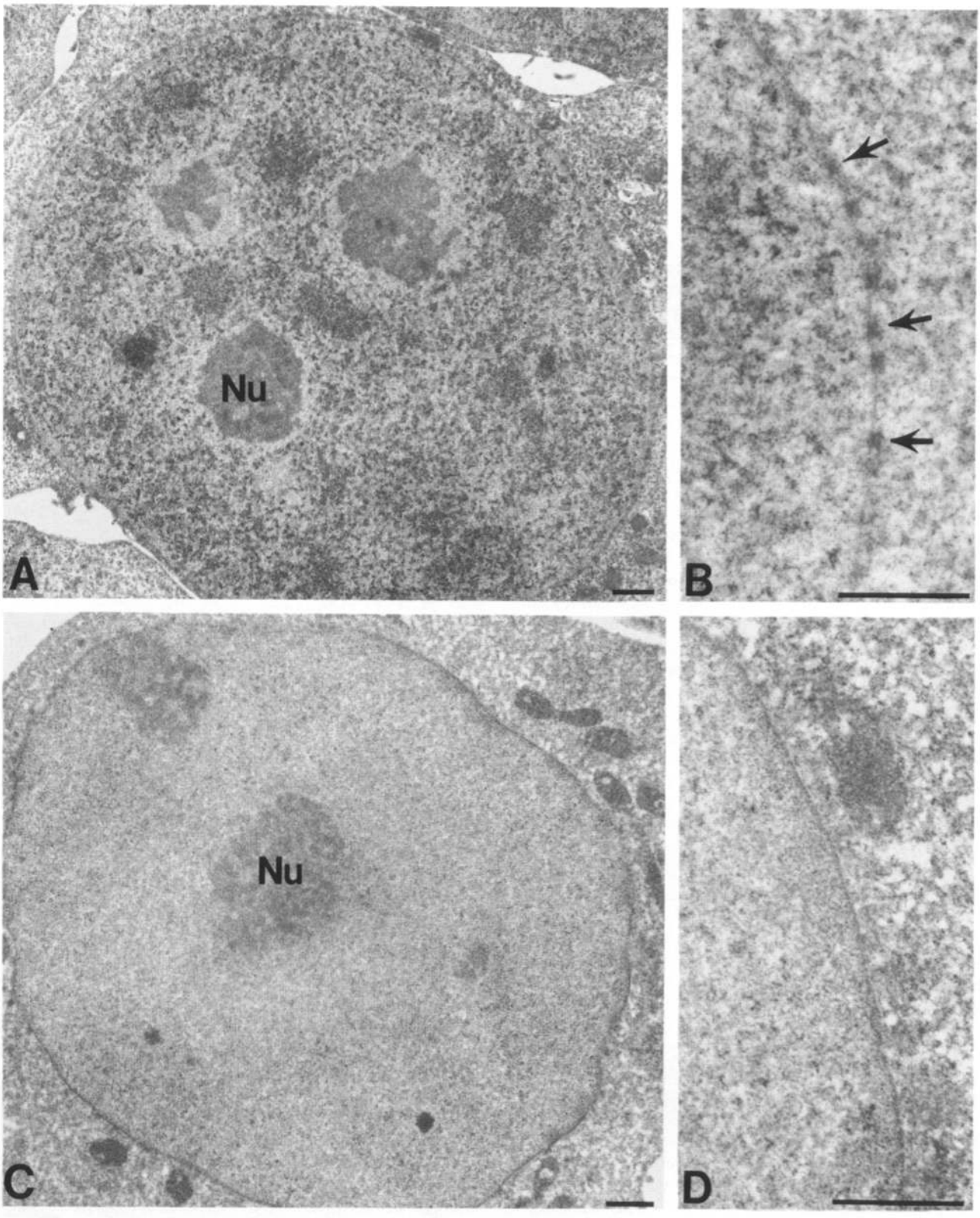

Figure 6. HeLa cells pretreated with DNAse I (100 U/ml for 2 h at 37°C) before hybridization resulted in a typical speckled labeling pattern (*A*) as compared to nontreated cells. The staining of poly(A)$^+$ RNA at the nuclear pore complexes (*arrows*) can be readily observed (*B*). Cells that were pretreated with RNAse T2 (100 U/ml for 2 h at 37°C) before hybridization showed no poly(A)$^+$ RNA labeling in either the nucleus (*C*) or the nuclear pore complexes (*D*). Cells were prepared by pre-embedding in situ hybridization with eosin photooxidation. Sections were not poststained. Bar, 1 μm.

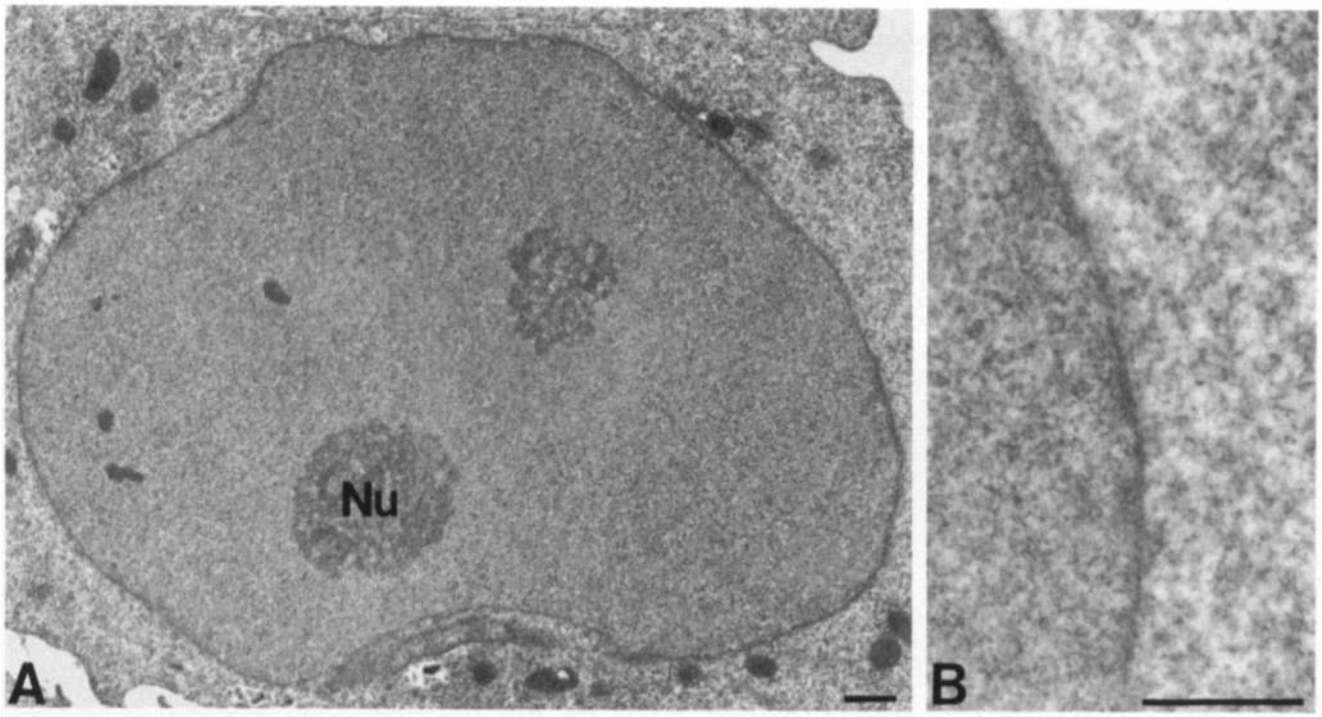

Figure 7. Cells were probed with biotin labeled $dA_{(50)}$ using the same conditions as with the biotin-labeled $dT_{(50)}$ probe. No staining was observed in either the nucleus (*A*) or the nuclear pore complexes (*B*) further confirming that the poly(A)$^+$ RNA staining by the oligo $dT_{(50)}$ probe was specific to poly(A)$^+$ RNA instead of random stickiness to other cellular constituents. Cells were prepared by pre-embedding in situ hybridization with eosin photooxidation. Sections were not poststained. Bar, 1 μm.

trated, larger, and fewer clusters (Fig. 11 *B*). These clusters were sensitive to RNase T2 digestion (data not shown). A similar reorganization was also observed in HeLa cells at both the light and electron microscopic level (Figs. 12 *A* and 13 *C*). These larger and fewer clusters have previously been identified as fused interchromatin granule clusters by electron microscopy (Spector et al., 1993). Observations of grazing sections show a reduced level of poly(A)$^+$ RNA at the nuclear pore complexes after the inhibition of transcription (Fig. 12 *B*). In addition to poly(A)$^+$ RNA, splicing factors in drug treated cells were also reorganized in an identical way (Fig. 13 *D*). Similar results were observed with the adenosine analog DRB, another drug which is known to cause early termination of 70–80% of pre-mRNA transcription (Tamm et al., 1978) (Fig. 11, *C* and *G*). However, the DRB effect is reversible. When cells were incubated in drug-free medium after the 3-h treatment, the speckled distribution of poly(A)$^+$ RNA began to recover within 30 min (Fig. 11, *D* and *H*). The recovery from the treatment with DRB excludes the possibility that the observed reorganization of splicing factors and poly(A)$^+$ RNA was simply due to cell death. These observations show that a population of poly(A)$^+$ RNA with a long half-life is associated with interchromatin granule clusters. While the amount of stable poly(A)$^+$ RNA present in interchromatin granule clusters seems to represent a significant pool of the total nuclear poly(A)$^+$ RNA, an accurate quantitative evaluation cannot be obtained in vivo as it has been shown that upon inhibition of transcription poly(A) tail length can increase (Brawerman and Diez, 1975).

To be sure that the effects observed with α-amanitin treatment were specifically due to the inhibition of RNA polymerase II and not to a secondary effect of the drug treatment, we performed similar experiments in a derivative CHO cell line, Amal, which is resistant to α-amanitin (Chan et al., 1972). This cell line contains a mutation in the gene coding for a polypeptide of RNA polymerase II (Ingles et al., 1976). The enzyme from mutant cells has a decreased affinity for binding α-amanitin. Ama 1 cells were incubated in up to 50 μg/ml of α-amanitin for the same period of time as CHO cells (5–7 h), and the distribution of poly(A)$^+$ RNA was examined. When compared to control cells which were not treated with drugs (Fig. 11 *E*), α-amanitin–treated cells showed no alteration in the distribution of poly(A)$^+$ RNA (Fig. 11 *F*) or in the level of transcription (Fig. 10 *F*). This finding supports the idea that the drug effect observed in non-resistant CHO cells is directly due to the inhibition of RNA polymerase II and not to a secondary effect of the drug treatment.

To rule out the possibility, that the observed stable population of poly(A)$^+$ RNA resulted from the inhibition of the synthesis of a labile protein whose function is necessary for RNA transport, we examined the effect of the protein synthesis inhibitor cycloheximide on the distribution pattern of poly(A)$^+$ RNA. It has been previously shown that the addition of cycloheximide for up to 10 h does not significantly alter transcription of pre-mRNA as monitored by [^{3}H]uridine incorporation (O'Keefe et al., 1994). Therefore, if poly(A)$^+$ RNA transport requires new protein synthesis, we would expect to see an accumulation of poly(A)$^+$ RNA in

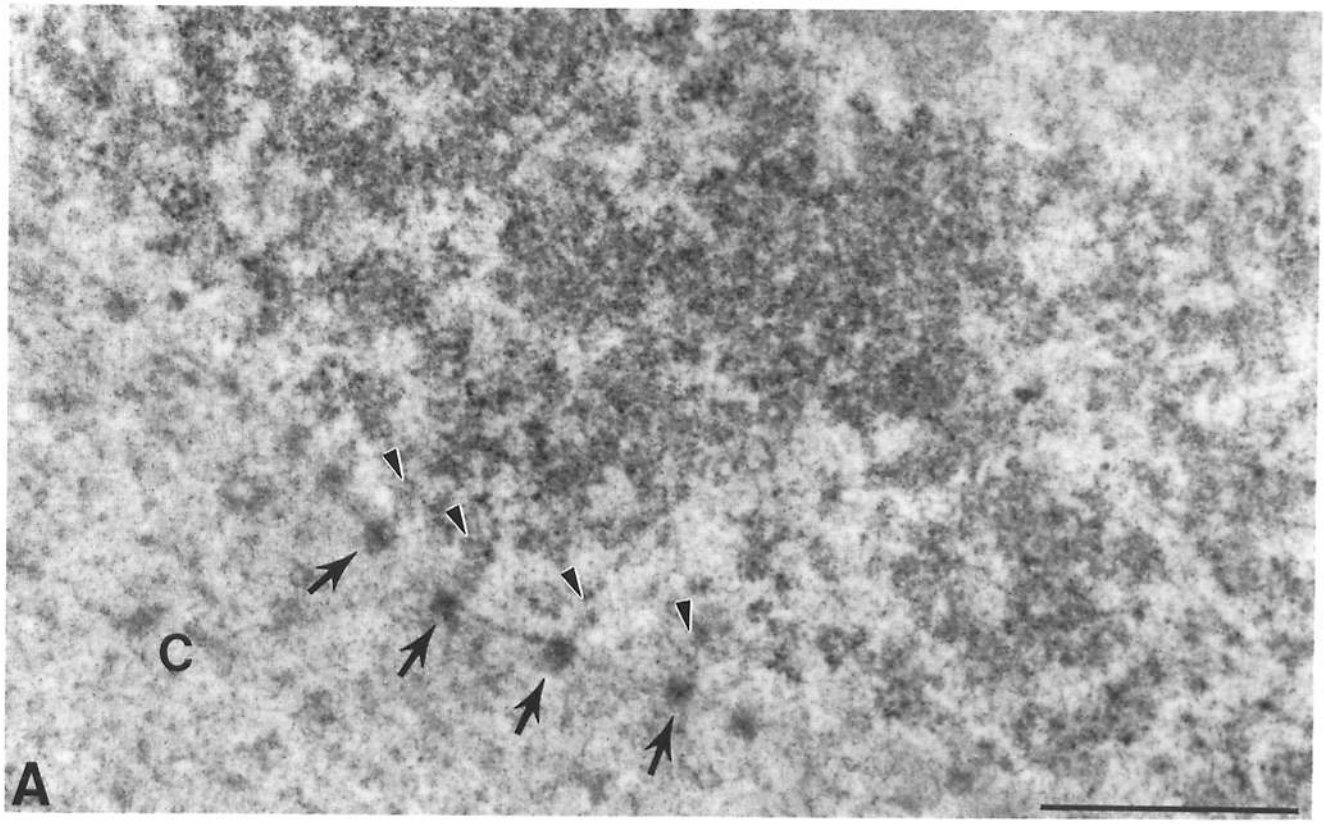

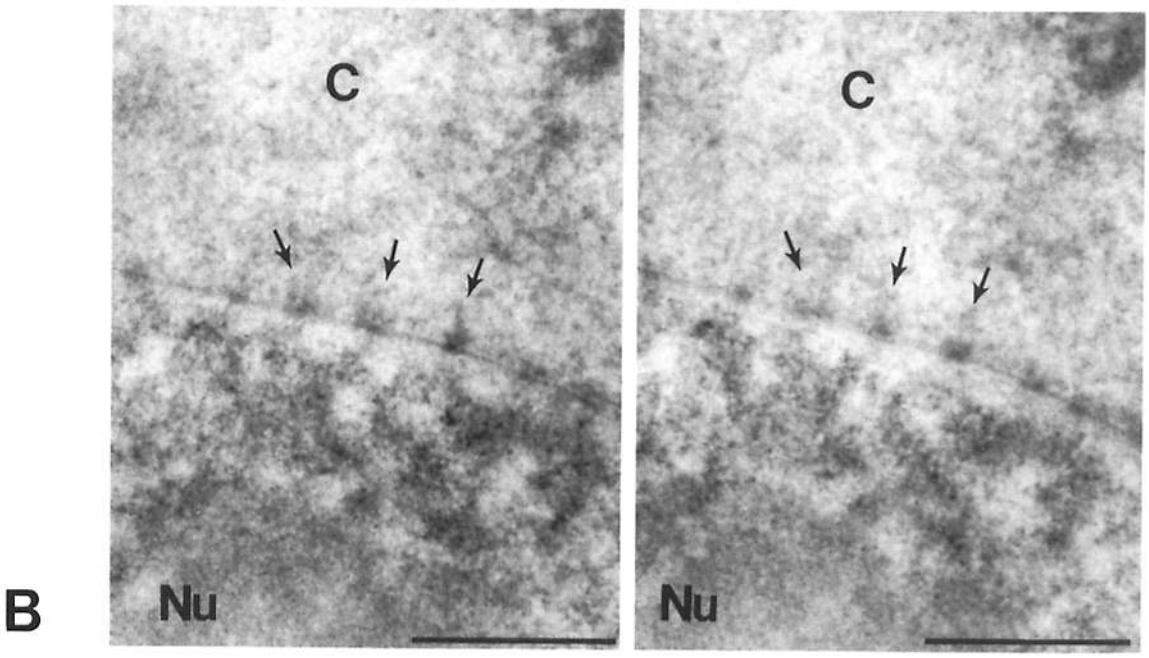

Figure 8. Transport of poly(A)$^+$ RNA through nuclear pore complexes is directly visualized at higher magnification by electron microscopic pre-embedding in situ hybridization with photooxidation. Poly(A)$^+$ RNA staining appears to taper into confined regions as it reaches the nuclear pore complexes (*A*, *arrowheads*). In addition a build-up of RNA is observed at the cytoplasmic side of the pore complex (*A*, *arrows*). Stereo images of 0.5-μm sections show in three dimensions the bridged localization of poly(A)$^+$ RNA between the intranuclear clusters and the nuclear pore complexes. Furthermore, ribbonlike structures, presumably representing RNA or RNPs, are observed leaving the nuclear pore complexes into the cytoplasm (*B*, *arrows*). Sections were not poststained. Bar, 1 μm.

Figure 9. Observation of poly(A)$^+$ RNA staining in nuclear pore complexes in grazing section by electron microscopic pre-embedding in situ hybridization with eosin photooxidation. Poly(A)$^+$ RNA is localized in all of the nuclear pore complexes (*A* and *B*) as compared to control cells which were not hybridized with the oligo $dT_{(50)}$ (*C*) suggesting that poly(A)$^+$ RNA is transported through all of the nuclear pores. Both experimental and control cells were processed under identical conditions. The poly(A)$^+$ RNA staining at the nuclear pore complexes appears to be concentrated around the periphery of the pore complexes when viewed at higher magnification (*B*). Sections were not poststained. Bar, 0.5 μm.

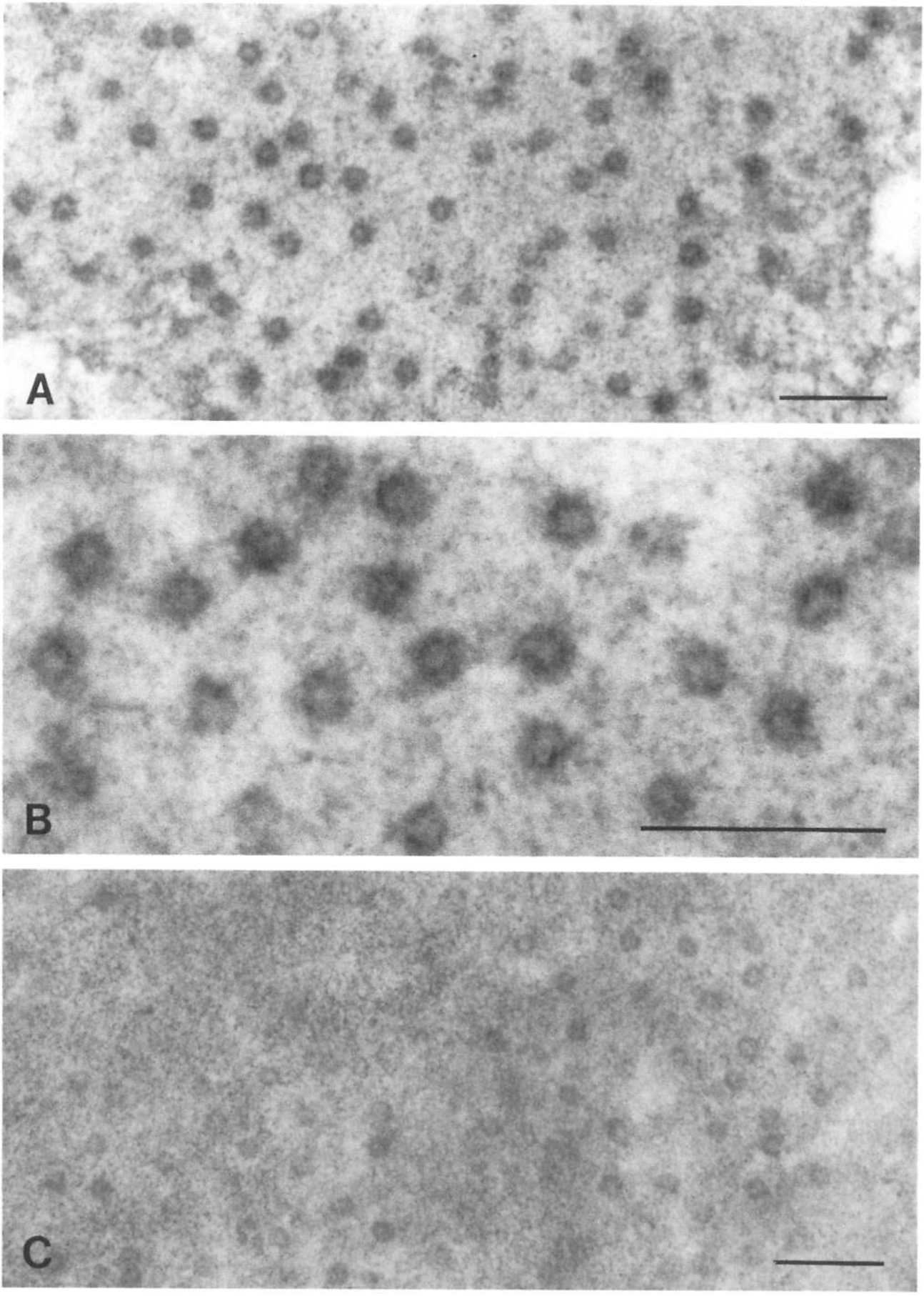

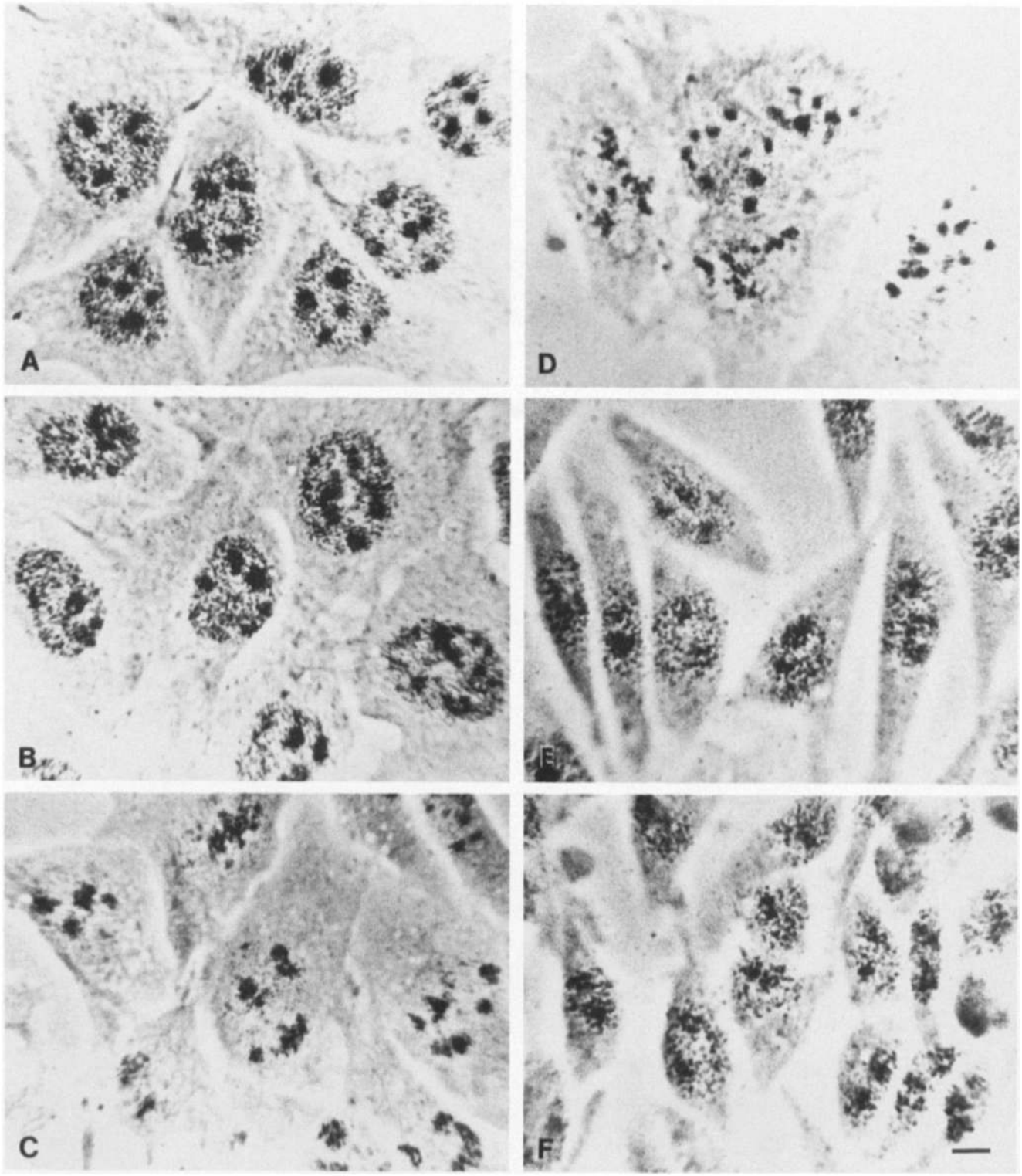

Figure 10. α-Amanitin inhibits the transcription of RNA polymerase II in CHO cells but not in Ama 1 cells. Transcription levels were monitored by [^{3}H]uridine incorporation. CHO cells which were not treated with α-amanitin exhibited autoradiographic grains over the nucleoli and throughout the nucleoplasm (*A*). Cells incubated with the α-amanitin (5 μg/ml) for 3 h (*B*) showed little change in the pattern of autoradiographic grains. After 5 h (*C*) to 24 h (*D*) of α-amanitin treatment, the number of autoradiographic grains present in the nucleoplasm decreased significantly. Control Ama 1 cells (*E*) and cells treated with α-amanitin (5 μg/ml) for 5 h (*F*) did not show a significant difference in the amount of [^{3}H]uridine labeling. Bar, 10 μm.

Figure 11. A fraction of poly(A)$^+$ RNA remains in the nucleus after transcription by RNA polymerase II is inhibited. When CHO cells were treated with α-amanitin (5 μg/ml) for 7 h, a significant amount of poly(A)$^+$ RNA was observed in the nuclei with an altered distribution (*B*) as compared to untreated cells (*A*). α-Amanitin treated Ama 1 cells showed little difference (*F*) as compared to nontreated cells (*E*). However, both CHO cells (*C*) and Ama 1 cells (*G*) are sensitive to the inhibition of RNA polymerase II by DRB and the observed changes are reversible after cells were incubated in DRB-free medium (*D* and *H*). Bar, 10 μm.

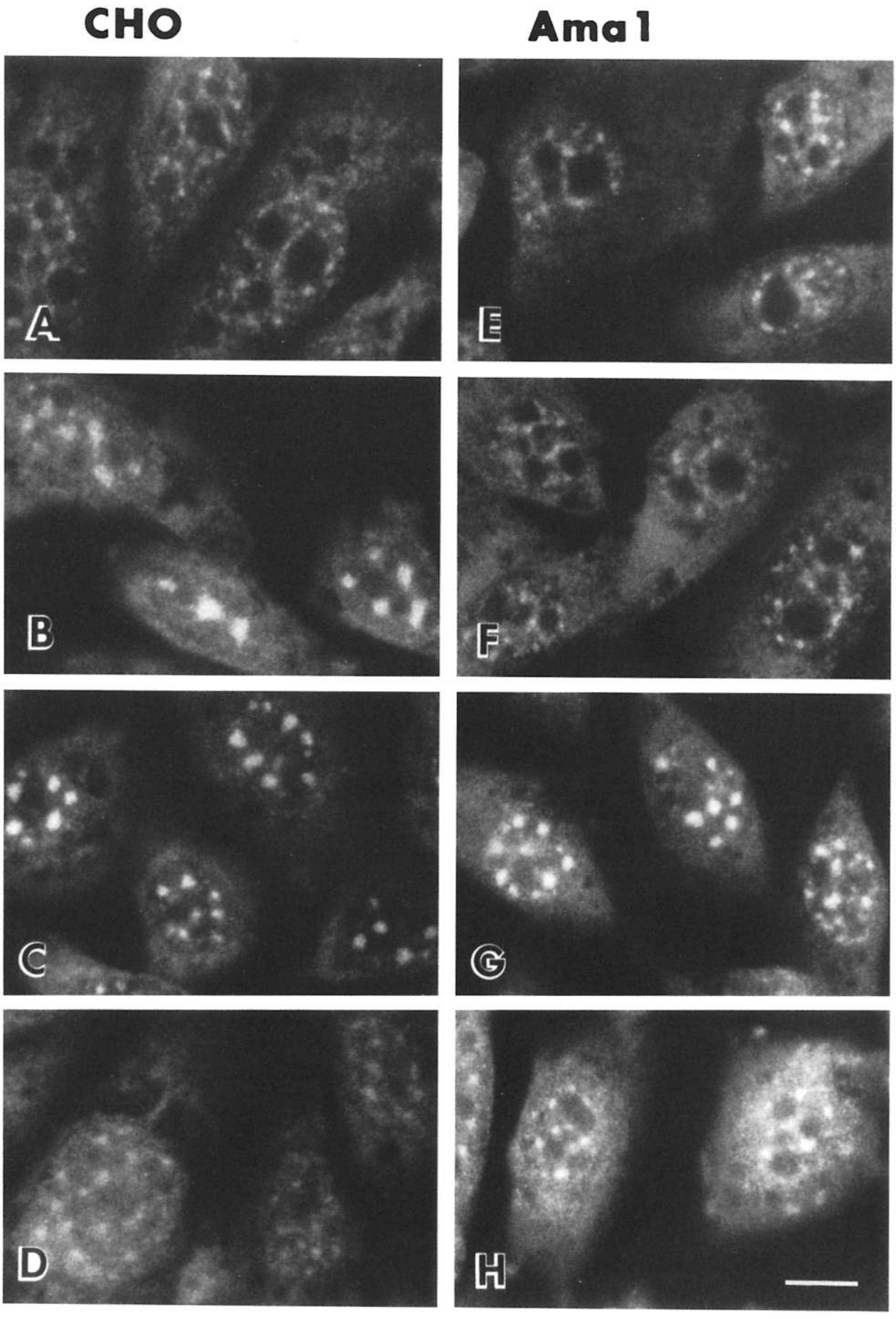

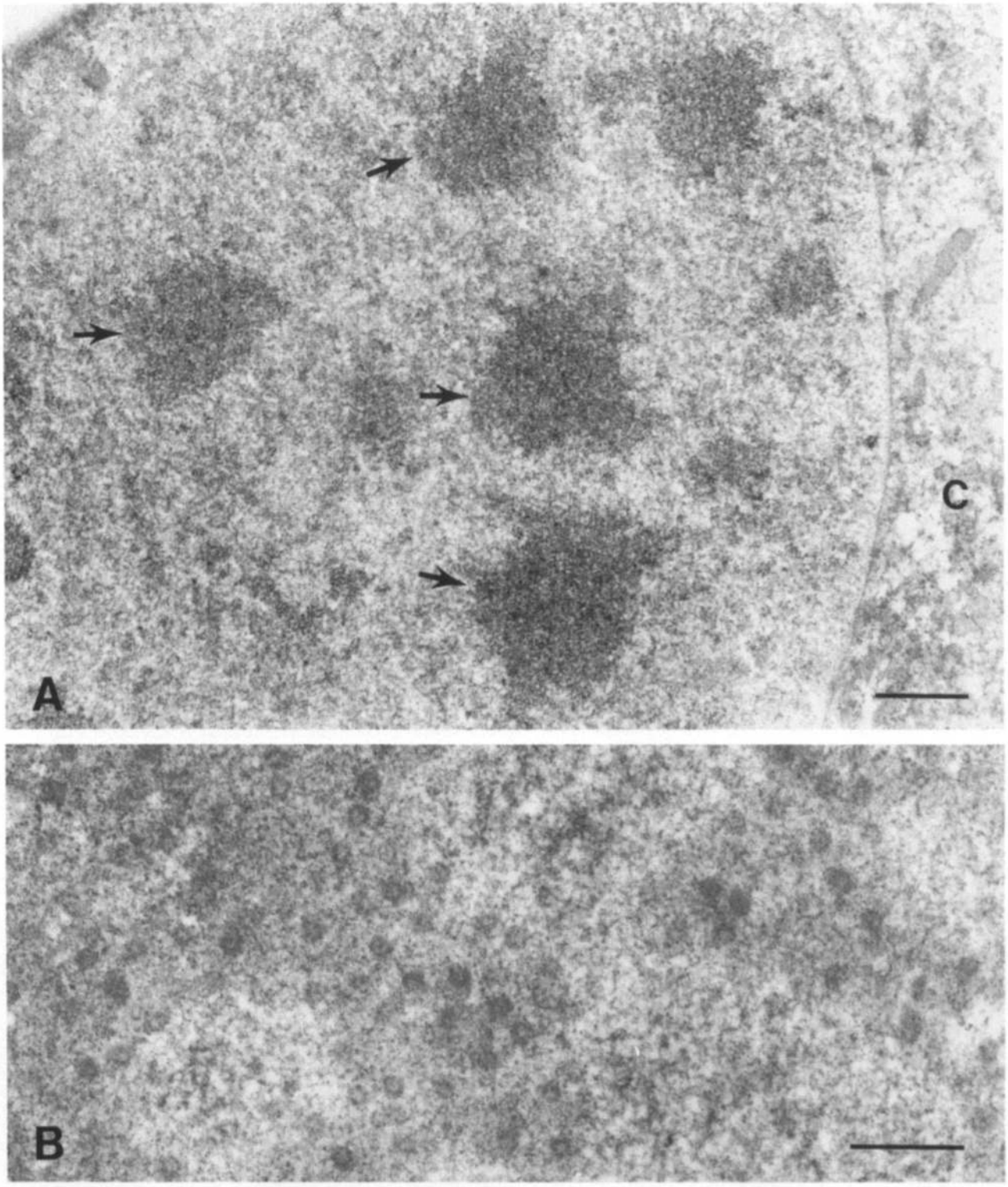

Figure 12. Poly(A)$^+$ RNA is reorganized into larger and fewer nuclear clusters when RNA polymerase II activity is inhibited by treatment of HeLa cells with 50 μg/ml α-amanitin for 7 h (*A*, *arrow*). However, the staining of poly(A)$^+$ RNA is still observed in some of the nuclear pores (*A*). When nuclear pore complexes are observed in grazing section, the intensity of poly(A)$^+$ RNA staining appears significantly decreased (*B*), but a subset of the pores are still labeled suggesting that the transport of poly(A)$^+$ RNA is not inhibited by inhibiting transcription. Cells were prepared by pre-embedding in situ hybridization with eosin photooxidation. Sections were not post-stained. Bar, 0.5 μm.

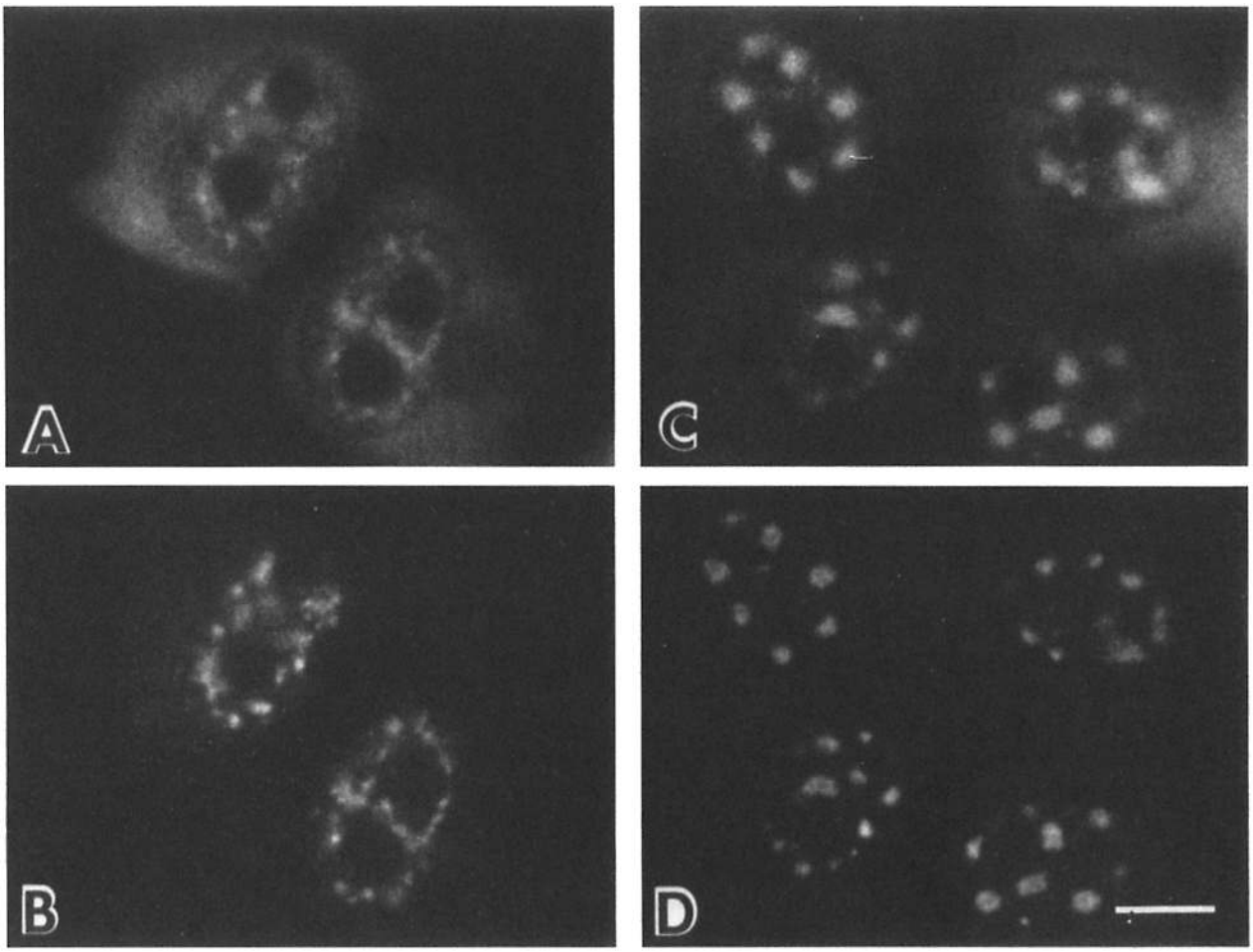

Figure 13. Upon inhibition of RNA polymerase II, pre-mRNA splicing factors were reorganized in a similar way as poly(A)$^+$ RNA. Actively transcribing HeLa cells (*A* and *B*) and cells treated with α-amanitin (*C* and *D*) were double labeled with an oligo $dT_{(50)}$ conjugated with FITC (*A* and *C*) and anti-SC35 antibody which was detected with Texas red–conjugated secondary antibodies (*B* and *D*). The distribution of both poly(A)$^+$ RNA and SC35 was reorganized into larger and fewer clusters and the connections between the clusters disappeared. Bar, 10 μm.

the nucleus after cells were treated with cycloheximide. However, both CHO and Ama 1 cells incubated with cycloheximide, at a concentration of 100 μg/ml for up to 5 h, did not show any obvious change in the speckled distribution of poly(A)$^+$ RNA (Fig. 14, *B* and *D*). This experiment demonstrated that protein synthesis was not required to maintain the speckled distribution pattern of poly(A)$^+$ RNA and that a labile protein was not involved in RNA transport. However, it is possible that transcription and transport of poly(A)$^+$ RNA may be tightly coupled so that the inhibition of transcription would inhibit RNA transport. We consider this possibility unlikely because it has previously been demonstrated that the transport of mRNA into the cytoplasm is independent of continuing RNA synthesis (Penman et al., 1970). In addition, we have observed a low level of poly(A)$^+$ RNA at the nuclear pore complexes after the inhibition of transcription, supporting the notion that transport has not been inhibited. It is, therefore most likely that a stable subpopulation of poly(A)$^+$ RNA resides in the nucleus, mostly in interchromatin granule clusters and does not serve as mRNA which will be transported to the cytoplasm for translation.

It is also possible that the poly(A)$^+$ RNA staining in the nucleus after inhibition of RNA polymerase II transcription represents RNA polymerase III transcripts. Previous studies have shown that 12–20% of newly synthesized poly(A)$^+$ RNA is transcribed by RNA polymerase III in murine tumor cells (Kramerov et al., 1990). To exclude the possibility that the poly(A)$^+$ RNA staining observed after CHO cells were treated with 5 μg/ml of α-amanitin is the result of transcription by RNA polymerase III, cells were incubated in α-amanitin at a concentration of 250 μg/ml which has been shown to inhibit RNA polymerase III activity (Kramerov et al., 1990). CHO cells were treated for up to 9.5 h and poly(A)$^+$ RNA localization was examined by in situ hybridization (Fig. 14 *E*). We have found that a substantial amount of poly(A)$^+$ RNA remains in the nucleus after drug treatment which is similar to the observation of cells treated with 5 μg/ml of α-amanitin. Therefore, we believe that the poly(A)$^+$ RNA in the nucleus observed upon inhibition of RNA polymerase

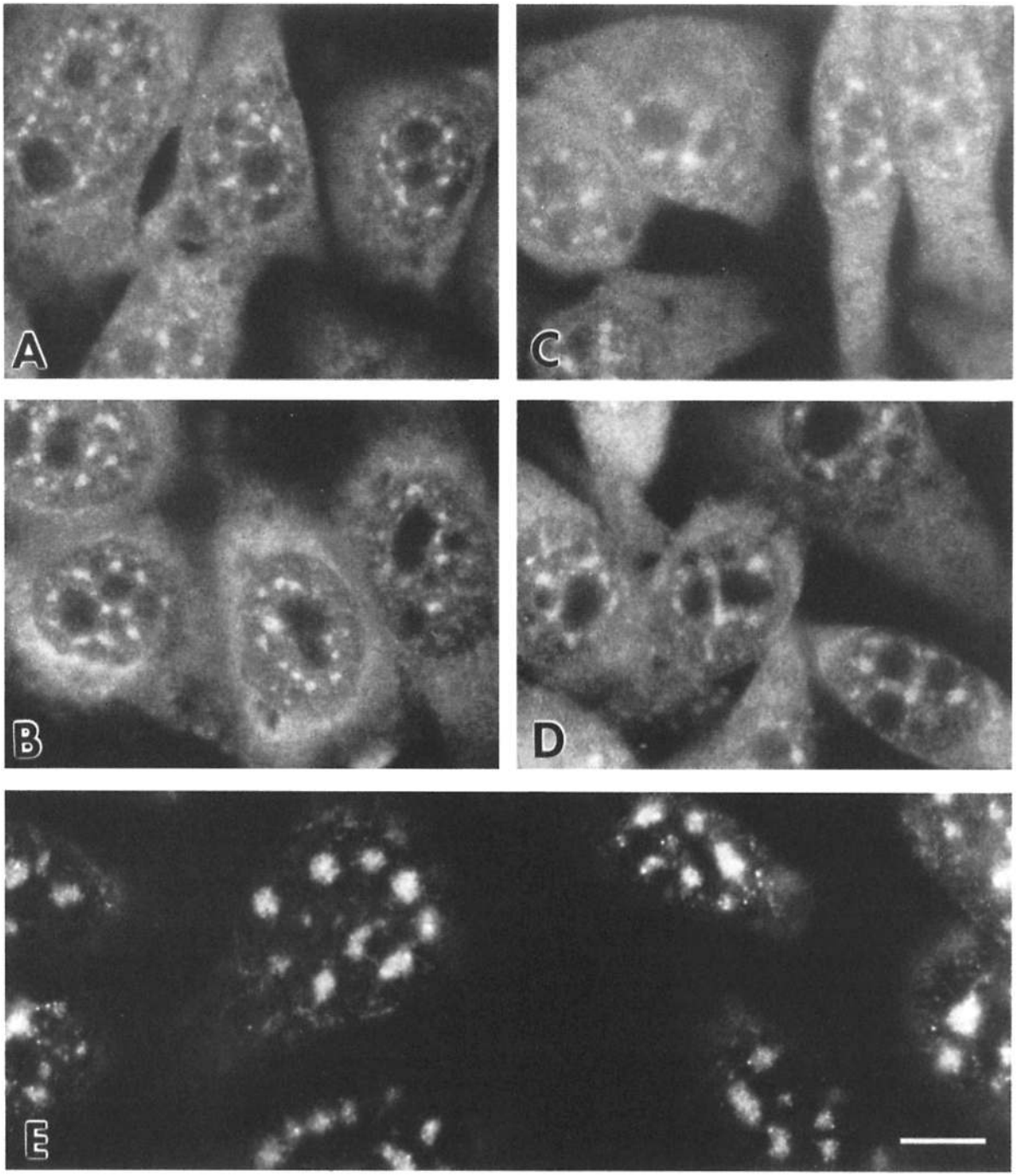

Figure 14. Protein synthesis is not required for RNA transport. Poly(A)$^+$ RNA staining did not increase in nuclei of cells treated with the protein synthesis inhibitor, cycloheximide. CHO cells (*A* and *B*) and Ama 1 cells (*C* and *D*) were treated (*B* and *D*) or not treated (*A* and *C*) with 100 μg/ml cycloheximide for 5 h. In addition, CHO cells were also treated with 250 μg/ml of α-amanitin to inactivate RNA polymerase III in addition to RNA polymerase II (*E*). Poly(A)$^+$ RNA was localized with an FITC-conjugated oligo $dT_{(50)}$ after cells were treated for 9.5 h. Poly(A)$^+$ RNA relocalized into fewer and larger clusters similar to what was observed when only RNA polymerase II activity was inhibited. Bar, 10 μm.

II is not the consequence of continuing production of RNA polymerase III transcripts, although it is possible that some stable RNA polymerase III transcripts which do not translocate to the cytoplasm are part of the poly(A)$^+$ RNA staining observed in interchromatin granule clusters.

Poly (A)$^+$ RNA Is Absent from Coiled Bodies

Coiled bodies belong to a group of structures called nuclear bodies. Coiled bodies contain an electron dense and a coiled granular structure when observed in the electron microscope. In addition to being enriched in p80 coilin (Chan et

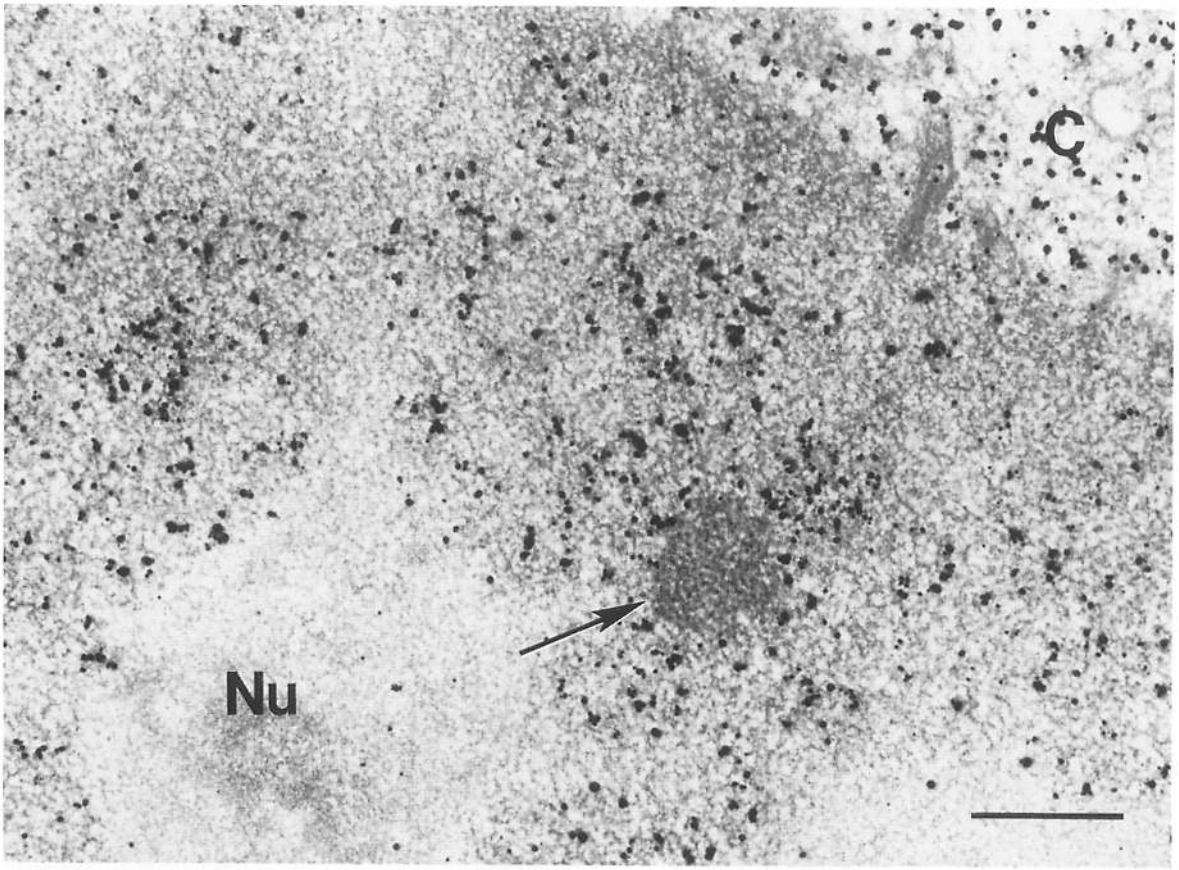

Figure 15. Coiled bodies contain little to no poly(A)$^+$ RNA. Poly(A)$^+$ RNA was localized in HeLa cells by pre-embedding gold labeling as described in the Materials and Methods. Poly(A)$^+$ RNA is localized in the nucleoplasm around the coiled body but it is not present within this nuclear structure (*arrow*). Bar, 1 μm.

al., 1989; Andrade et al., 1993; Raska et al., 1991), coiled bodies contain many components which are required for pre-mRNA and rRNA processing such as U1-U6 snRNPs and fibrillarin (Carmo-Fonseca et al., 1991*a*,*b*; Raska et al., 1991; Huang and Spector, 1992; Spector et al., 1992). Coiled bodies have been more commonly found in tumor and transformed cells, but can also be found less frequently in certain normal cells such as neurons and liver cells (Ramon y Cajal, 1903; Fakan et al., 1984). However, only a very small percentage (2–4%) of primary fibroblasts contain these structures. The functional significance of coiled bodies is unknown. Since coiled bodies contain many known RNA processing factors, they were proposed to be involved in pre-mRNA splicing, or in storage and/or recycling of splicing factors (Carmo-Fonseca et al., 1991*a*,*b*, 1992). If coiled bodies are directly involved in pre-mRNA splicing, we would expect to see poly(A)$^+$ RNA in these structures. To test this possibility, pre-embedding in situ hybridization was performed using an oligo $dT_{(50)}$ probe and little to no labeling of poly(A)$^+$ RNA was found in coiled bodies (Fig. 15).

Discussion

We have examined the subnuclear localization of poly(A)$^+$ RNA by electron microscopic in situ hybridization. We have found that poly(A)$^+$ RNA localizes in the nucleus in a speckled pattern which corresponds to both interchromatin granule clusters and perichromatin fibrils and which is associated with the nuclear matrix. When RNA polymerase II transcription is inhibited for up to 10 h, a stable population of poly(A)$^+$ RNA remains in the interchromatin granule clusters which fuse into fewer and larger clusters. In addition, we have visualized for the first time in mammalian cells the nuclear poly(A)$^+$ RNA coming into direct contact with nuclear pore complexes. We have also visualized the transport of poly(A)$^+$ RNA through the nuclear pore complexes.

Nuclear Organization and Poly(A)$^+$ RNA Localization

The function and organization of cytoskeletal elements such as microfilaments, microtubules, and intermediate filaments in the cytoplasm has been studied extensively both in vivo and in vitro. However, much less information is available as to the basic structural components involved in nuclear architecture. Early studies at the light microscopic level (Smetana et al., 1963) and later studies at the electron microscopic level identified a RNP network which contains components that are present in the nuclear matrix (Berezney and Coffey, 1974). The use of RNase inhibitors and ammonium sulfate extraction significantly improved the preservation of the RNP network in nuclear matrix preparations (Fey et al., 1986; Smith et al., 1986; Belgrader et al., 1991). When such samples were observed in an embedment-free medium at the electron microscopic level an elaborate arrangement of 10-

nm core filaments was seen (Fey et al., 1986; He et al., 1990). However, such filaments have thus far not been observed in intact nuclei. Nevertheless, EDTA regressive staining of unextracted cells revealed a contiguous, ribonucleoprotein containing "interchromatin net" (Puvion and Bernhard, 1975) which may be a part of the nuclear matrix. The nuclear matrix has been shown to contain hnRNA (Ciejek et al., 1982; Mariman et al., 1982), splicing components such as snRNPs (Vogelstein and Hunt, 1982; Spector et al., 1983; Smith et al., 1986), as well as functional spliceosomes (Zeitlin et al., 1987, 1989). In fact, the integrity of the structure is dependent upon the preservation of RNA components (van Eekelen and van Venrooij, 1981; Long and Schrier, 1983; Bouvier et al., 1985; He et al., 1990). Some of the protein components of the matrix have been characterized. One recent example is nuclear-mitotic apparatus protein (NuMA), which has been found to be associated with the nuclear matrix in interphase cells and the mitotic apparatus during mitosis (Zeng et al., 1994). The association with microtubules during mitosis suggests that NuMA may be part of or associated with the filamentous nuclear scaffold. The nuclear matrix has been proposed to play an important role in many nuclear functions such as DNA replication, transcription and mRNA metabolism (for a review see Berezney 1991). Supporting evidence for the interaction of newly synthesized RNA with the nuclear matrix comes from the work of Xing and Lawrence (1991) who showed that Epstein Barr Virus primary transcripts were present in nuclear matrix preparations from Namalwa cells. In the present study, we have shown that the majority of poly(A)$^+$ RNA is closely associated with the nuclear matrix. Therefore, it is very likely that poly(A)$^+$ RNA becomes attached to the nuclear matrix upon transcription.

A Stable Population of Poly(A)$^+$ RNA May Be Important for Nuclear Function

There are at least two possible explanations for the presence of large amounts of poly(A)$^+$ RNA in interchromatin granule clusters which are not actively involved in transcription. First, the poly(A)$^+$ RNA present in these regions may represent RNA which is in transit to the nuclear envelope. However, this seems unlikely since these nuclear regions do not label with [^{3}H]uridine in a short pulse. A higher frequency of labeling of interchromatin granule clusters was observed in cells labeled for 6 h followed by a chase of 24 h (Fakan and Bernard, 1973). Therefore, the [^{3}H]uridine incorporation data are not consistent with a pathway of poly(A) that goes from perichromatin fibrils to interchromatin granule clusters to the cytoplasm. A second possibility is that the poly(A)$^+$ RNA which is found in the interchromatin granule clusters does not represent pre-mRNA, but instead represents a stable RNA population involved in other nuclear functions. Evidence to support this possibility comes from early biochemical studies which showed a considerable amount of nuclear poly(A)$^+$ RNA to be a component of large stable nuclear RNAs (Herman et al., 1976; Brawerman and Diez, 1975; Perry et al., 1974). Furthermore, it was found that a significant fraction of nuclear poly(A)$^+$ RNA consisted of sequences which were not detected in the cytoplasm (Herman et al., 1976). Two recent examples have been found of specific polyadenylated RNAs which remain in the nucleus. The first example is the XIST gene transcript from the inactivated human X chromosome (Brockdorff et al., 1992; Brown et al., 1992). It is estimated that 98.8% of the Xist transcripts, which are polyadenylated, remain in the nucleus (Brockdorff et al., 1992). In situ hybridization has localized the XIST transcripts to the inactivated X chromosome (Brown et al., 1992). However, a recent study has shown that this RNA is not involved in maintaining the inactivation of the X chromosome (Brown and Willard, 1994). In the second example, Hogan et al. (1994) have reported that one of the major transcripts of the *Hsr-omega* gene in *Drosophila*, the Omega-n transcript, is unspliced, polyadenylated and remains in the nucleus of cells. These examples leave open the possibility that other chromosomes may also produce polyadenylated RNAs which remain in the nucleus and function in chromatin regulation and/or nuclear structure. Studies are currently underway to biochemically identify the stable nuclear poly(A)$^+$ RNA species.

Not only does the stable poly(A)$^+$ RNA remain in the nucleus after cells are treated with transcription inhibitors, but the organization of these RNAs in the nucleus also changes. Instead of the typical speckled localization pattern, poly(A)$^+$ RNA concentrates into fewer and larger interchromatin granule clusters. Correspondingly, splicing factors such as snRNPs and SC35 also changed their distribution into the same structures. Accompanying the fusion of interchromatin granule clusters, perichromatin fibrils between the clusters decrease significantly. A similar reorganization of RNP elements has been previously observed upon drug treatment of cells (Brasch, 1989). The cause of such a reorganization is unclear, however, several recent studies have shown that depletion of splicing activity may result in such a reorganization. Microinjection into cells of oligonucleotides or antibodies which inhibit pre-mRNA splicing in vitro showed that splicing factors were reorganized into fewer and larger interchromatin granule clusters (O'Keefe et al., 1994). A similar rearrangement of splicing factors was also previously observed in cells infected with herpes simplex virus (Martin et al., 1987; Phelan et al., 1993). In this case, the virus produces a large population of RNAs which are not spliced. All of these observations suggest that the typical speckled organization of splicing factors and poly(A)$^+$ RNA is dependent upon the transcriptional and pre-mRNA splicing activities of the cell. Upon inhibition of one or both of these functions, the structural organization of the nucleus is changed to reflect alterations in functional activity. In addition, these observations further support the hypothesis that interchromatin granule clusters (the larger speckles) are likely to be storage and/or reassembly sites of splicing factors whereas perichromatin fibrils (connections between speckles and diffuse nuclear labeling) are the sites of active transcription. The poly(A)$^+$ RNA in the interchromatin granule clusters does not represent nascent RNA transcripts, but instead represents a stable RNA population which may play an important role in nuclear function.

Poly(A)$^+$ RNA Is Not Present in Coiled Bodies

Electron microscopic in situ hybridization has clearly demonstrated that coiled bodies contain little to no poly(A)$^+$ RNA. These data taken together with previous studies which have shown that coiled bodies contain little to no [^{3}H]uridine labeling, ssDNA or dsDNA, RNA polymerase II, or SC35 (for a review see Spector, 1993) make it unlikely that

these nuclear structures are the sites of active pre-mRNA splicing. In addition, coiled bodies are present in only a small percentage (2–4%) of cells of certain cell types such as primary human fibroblasts suggesting that coiled bodies are not essential for cellular function. However, in transformed cells, coiled bodies are significantly larger and more abundant (80–99% of the population) (Spector et al., 1991) suggesting that the presence of coiled bodies may be a reflection of the physiological condition of the cells. The enrichment of major snRNPs in coiled bodies raises the possibility that coiled bodies are involved in the reassembly or recycling of major snRNPs or are a result of altered transcription in these cells (for a review see Brasch and Ochs, 1992; Lamond and Carmo-Fonseca, 1993).

Transport of Poly(A)$^+$ RNA from the Nucleus to the Cytoplasm

There has been relatively little information available as to how RNA transcripts are transported from their sites of transcription to the nuclear envelope. There are at least two possible mechanisms that can be explored. First, newly made RNAs may be processed and move through the nucleus by simple diffusion. Evidence supporting this hypothesis comes from a recent report on RNA transport in the salivary gland nuclei of Drosophila third instar larvae (Zachar et al., 1993). In this study, hybridization to a highly expressed chimeric transcript has revealed an intense hybridization signal at the site of transcription and a less intense signal which forms an interchromosomal channel network throughout the nucleoplasm. SnRNPs were also localized within this network. Based on this localization the authors have proposed that RNAs move through the interchromosomal channel network by diffusion.

The second possible mechanism is that RNAs are actively transported through the nucleus in a directed manner. Several studies have provided data which are consistent with this possibility. First, transport of mRNA in Xenopus oocytes can be inhibited by alteration of the 5′ cap structure and by placing cells at 4°C suggesting that a specific signal is required and that the transport process is energy dependent (Schroder et al., 1989; Hamm and Mattaj, 1990; Dargemont and Kuhn, 1992). The 3′ end formation of mRNA has also been found to be important for mRNA export to the cytoplasm in mammalian cells (Eckner et al., 1991). Secondly, treatment of mammalian cells with the actin depolymerizing drug cytochalasin D or injection of specific anti-actin antibodies into mammalian cell nuclei results in a block of RNA transport suggesting that actin or actin-like proteins in the nucleus are essential for the transport process (Schindler and Jiang, 1986). Furthermore, the association of poly(A)$^+$ RNA as well as specific RNA species (Xing and Lawrence, 1991) with the nuclear matrix suggests an intimate interaction of nascent RNA transcripts with nuclear structures and indicates that many RNAs are not soluble as one might expect if they were being transported by diffusion. All of these observations seem to favor the possibility that an active mechanism is involved in the transport of RNA through the nucleus. The direct visualization of poly(A)$^+$ RNA export to and through the nuclear pore complex in this report further supports the possibility of active transport. The observation shows that nuclear regions enriched in poly(A)$^+$ RNA taper as they approached the nuclear pore complexes. It is very tempting to speculate that the mature mRNP moves along nuclear filaments which lead to the nuclear pores. A recent study (Cordes et al., 1993) which examined a specific nuclear pore complex protein provides the foundation for such speculation. A 190-kD nuclear pore complex protein was found to be able to assemble into filamentous structures of 3–6 nm in diameter which extended into the nucleoplasm. The length of the filaments exceeded the length of the inner annulus–associated filamentous "cage" described in recent models of the nuclear pore complex (Jarnik and Aebi, 1991; Ris, 1991). These filaments were also observed bridging nucleoli and other parts of the nucleus to the nuclear pore complex (Cordes et al., 1993). Because of the similarity of the localization of p190 and poly(A)$^+$ RNA labeling, these filaments are ideal candidates for providing the framework for RNA transport into the nuclear pore complex. Furthermore, the 8–10-nm core filaments previously identified as components of the nuclear matrix (He et al., 1990) and/or the 9–10-nm nuclear–cytoplasmic filaments observed in whole cells by high voltage electron microscopy (Ellisman, 1987) may also provide a framework for such transport.

When examining the poly(A)$^+$ RNA labeling of the nuclear pores in cross-section, it was noticed that the central region of the pore complex was less intensely stained than the periphery resulting in a doughnut-shaped localization pattern. Nuclear pores have been extensively characterized in three-dimensions (Ris, 1989, 1991; Jarnik and Aebi, 1991; Goldberg and Allen, 1992; Hinshaw et al., 1992). The center of the pore is composed of a plug which extends through the long axis of the pore. This plug is thought to represent a transporter which facilitates the exchange between the nucleus and the cytoplasm (Akey and Goldfarb, 1989). The donut shaped staining could be explained such that the less intensely stained center represents a transporter molecule which behaves as a motor or interacts with the motor on the mRNP to move the RNP through the space between the periphery of the nuclear pore complex and the transporter. However, we are also aware of the possibility that under the low stringency fixation condition used in the present study, the ultrastructure of the pore complexes may not be well preserved and so the peripheral staining may be due to collapse of structure within the pore complex. Future studies will attempt to examine this possibility more closely.

Poly(A)$^+$ RNA appears to label the nuclear pore complexes most heavily on their cytoplasmic side suggesting that a rate limiting step in RNA transport occurs at this point of the nuclear pore complex. The latest studies of the nuclear pore structure have shown that eight highly twisted filaments project from the ring of the pore into the cytoplasm (Ris, 1991). It is therefore possible that these filaments are involved in the final release of RNA or RNP into the cytoplasm. It is also possible that the release of RNA or RNP to the cytoplasm is coupled with the binding of the RNA to free ribosomes and the rough endoplasmic reticulum both of which are localized in the vicinity of the nuclear envelope. The coupling of RNA transport and translation has been suggested in the case of the Balbiani ring gene transcripts in salivary gland cells of *Chironomus tentans* (Mehlin et al., 1992). The large size of the Balbiani ring RNP (50 nm) allows for a direct visualization of its movement through the nuclear pore complex to the cytoplasm. The RNA component (37 kb) was found to unwind at the pore complex and

the extended 5′ end of the transcript was observed to be associated with ribosomes in the cytoplasm while the 3′ end of the transcript still remained in the nuclear pore complex (Mehlin et al., 1991, 1992).

Our observation of the association of poly(A)$^+$ RNA with all of the nuclear pore complexes agrees with previous microinjection studies (Feldherr and Akin, 1990) which showed that all of the pores are capable of exporting RNA. In addition, Dworetzky and Feldherr (1988) showed that an individual nuclear pore is capable of both protein import and RNA export. The possibility of detecting specific cellular RNAs in the nucleus at the electron microscopic level will allow us to determine whether transcripts from individual genes are transported through all or a subset of nuclear pores. If only a subset of the pores are involved in transport of certain transcripts, as has been suggested by the gene-gating hypothesis (Blobel, 1985), it will be interesting to determine the spatial relationship of the localization of the gene to the nuclear pores involved in the transport of its RNA.

We thank Robert Derby and Shelley Kaurin for expert technical assistance. We are grateful to Scott Henderson, Ray O'Keefe, and Tokio Tani for helpful comments and discussions. We thank Xiang-Dong Fu (University of California, San Diego) for anti-SC35 antibody and Rick Powell of Nanoprobes Inc. (Stony Brook, NY) for FITC-conjugated 1.4-nm gold.

This work was supported by grants from the National Institutes of Health (GM42694 and 5P30 CA45508-04) to D.L. Spector and (RR 04050 and NS26739) to M.H. Ellisman.

Received for publication 21 February 1994 and in revised form 16 May 1994.

References

Akey, C. W., and D. S. Goldfarb. 1989. Protein import through the nuclear pore complex is a multistep process. *J. Cell Biol.* 109:971–982.

Andrade, L. E. C., E. M. Tan, and E. K. L. Chan. 1993. Immunocytochemical analysis of the coiled body in the cell cycle and during cell proliferation. *Proc. Natl. Acad. Sci. USA.* 90:1947–1951.

Belgrader, P., A. J. Siegel, and R. Berezney. 1991. A comprehensive study on the isolation and characterization of the HeLa S3 nuclear matrix. *J. Cell Sci.* 98:281–291.

Berezney, R., and D. S. Coffey. 1974. Identification of a nuclear protein matrix. *Biochem. Biophys. Res. Commun.* 60:1410–1419.

Berezney, R. 1991. The nuclear matrix: a heuristic model for investigating genomic organization and function in the cell nucleus. *J. Cell. Biochem.* 47:109–123.

Bernhard, W. 1969. A new staining procedure for electron microscopical cytology. *J. Ultrastruc. Res.* 27:250–265.

Blobel, G. 1985. Gene gating: a hypothesis. *Proc. Natl. Acad. Sci. USA.* 82:8527–8529.

Bouvier, D., J. Hubert, A.-P. Seve, and M. Bouteille. 1985. Structural aspects of intranuclear matrix disintegration upon RNase digestion of HeLa cell nuclei. *Eur. J. Cell Biol.* 36:323–333.

Brasch, K. 1989. Drug and metabolite-induced perturbations in nuclear structure and function: a review. *Biochem. Cell. Biol.* 68:408–426.

Brasch, K., and R. L. Ochs. 1992. Nuclear bodies (NBs): a newly "rediscovered" organelle. *Exp. Cell Res.* 202:211–223.

Brawerman, G., and J. Diez. 1975. Metabolism of the polyadenylate sequence of nuclear RNA and messenger RNA in mammalian cells. *Cell.* 5: 271–280.

Brockdorff, N., A. Ashworth, G. F. Kay, V. M. McCabe, D. P. Norris, P. J. Cooper, S. Swift, and S. Rastan. 1992. The product of the mouse Xist gene is a 15 kb inactive X-specific transcript containing no conserved ORF and located in the nucleus. *Cell.* 71:515–526.

Brown, C. J., and H. F. Willard. 1994. The human X-inactivation centre is not required for maintenance of X-chromosome inactivation. *Nature (Lond.).* 368:154–156.

Brown, C. J., B. D. Hendrich, J. L. Rupert, R. G. Lafreniere, Y. Xing, J. Lawrence, and H. F. Willard. 1992. The human XIST gene: analysis of a 17 kb inactive X-specific RNA that contains conserved repeats and is highly localized within the nucleus. *Cell.* 71:527–542.

Carmo-Fonseca, M., R. Pepperkok, B. S. Sproat, W. Ansorge, M. S. Swanson, and A. I. Lamond. 1991a. *In vivo* detection of snRNP-rich organelles in the nuclei of mammalian cells. *EMBO (Eur. Mol. Biol. Organ.) J.* 10:1863–1873.

Carmo-Fonseca, M., D. Tollervey, R. Pepperkok, S. M. L. Barabino, A. Merdes, C. Brunner, P. D. Zamore, M. R. Green, E. Hurt, and A. I. Lamond. 1991b. Mammalian nuclei contain foci which are highly enriched in components of the pre-mRNA splicing machinery. *EMBO (Eur. Mol. Biol. Organ.) J.* 10:195–206.

Carmo-Fonseca, M., R. Pepperkok, M. T. Carvalho, and A. I. Lamond. 1992. Transcription-dependent colocalization of the U1, U2, U4/U6 and U5 snRNPs in coiled bodies. *J. Cell Biol.* 117:1–14.

Carter, K. C., K. L. Taneja, and J. B. Lawrence. 1991. Discrete nuclear domains of poly(A) RNA and their relationship to the functional organization of the nucleus. *J. Cell Biol.* 115:1191–1202.

Carter, K. C., D. Bowman, W. Carrington, K. Fogarty, J. A. McNeil, F. S. Fay, and J. B. Lawrence. 1993. A three-dimensional view of precursor messenger RNA metabolism within the mammalian nucleus. *Science (Wash. DC).* 259:1330–1335.

Chan, V. L., G. F. Whitmore, and L. Siminovitch. 1972. Mammalian cells with altered forms of RNA polymerase II. *Proc. Natl. Acad. Sci. USA.* 69: 3119–3123.

Chan, E. K. L., K. F. Sullivan, and E. M. Tan. 1989. Ribonucleoprotein SS-B/La belongs to a protein family with consensus sequences for RNA-binding. *Nucleic Acids Res.* 17:2233–2244.

Ciejek, E. M., J. L. Nordstrom, M.-J. Tsai, and B. W. O'Malley. 1982. Ribonucleic acid precursors are associated with the chick oviduct nuclear matrix. *Biochemistry.* 21:4945–4953.

Cordes, V. C., S. Reidenbach, A. Kohler, N. Stuurman, R. van Driel, and W. W. Franke. 1993. Intranuclear filaments containing a nuclear pore complex protein. *J. Cell Biol.* 123:1333–1344.

Dargemont, C., and L. C. Kuhn. 1992. Export of mRNA from microinjected nuclei of *Xenopus laevis* Oocytes. *J. Cell Biol.* 118:1–9.

Deerinck, T. J., M. E. Martone, V. Lev Ram, D. Greene, R. Y. Tsien, D. L. Spector, S. Huang, and M. H. Ellisman. 1994. Fluorescence photooxidation with eosin-5-isothiocyanate: a method for high resolution immunolocalization and in situ hybridization for light and electron microscopy. 126: 901–910.

Dworetzky, S. I., and C. M. Feldherr. 1988. Translocation of RNA-coated gold particles through the nuclear pores of oocytes. *J. Cell Biol.* 106:575–584.

Eckner, R., W. Ellmeier, and M. L. Birnstiel. 1991. Mature mRNA 3′ end formation stimulates RNA export from the nucleus. *EMBO (Eur. Mol. Biol. Organ.) J.* 10:3513–3522.

Ellisman, M. H. 1987. Transcellular filament system. *In* Encyclopedia Neuroscience. Vol. II. G. Adelman, editor. Birkhauser Boston, Inc., Cambridge, MA. 1232–1233.

Fakan, S., and W. Bernhard. 1973. Nuclear labeling after prolonged 3H-uridine incorporation as visualized by high resolution autoradiography. *Exp. Cell Res.* 79:431–444.

Fakan, S., and E. Puvion. 1980. The ultrastructural visualization of nucleolar and extranucleolar RNA synthesis and distribution. *Int. Rev. Cytol.* 65:255–299.

Fakan, S., G. Leser, and T. E. Martin. 1984. Ultrastructural distribution of nuclear ribonucleoproteins as visualized by immunocytochemistry on thin sections. *J. Cell Biol.* 98:358–363.

Feldherr, C. M., and D. Akin. 1990. EM visualization of nucleocytoplasmic transport processes. *Electro Microsc. Rev.* 3:73–86.

Fey, E. G., G. Krochmalnic, and S. Penman. 1986. The nonchromatin substructures of the nucleus: the ribonucleoprotein (RNP)-containing and RNP-depleted matrices analyzed by sequential fractionation and resinless section electron microscopy. *J. Cell Biol.* 102:1654–1665.

Fu, X.-D., and T. Maniatis. 1990. Factor required for mammalian spliceosome assembly is localized to discrete regions in the nucleus. *Nature (Lond.).* 343:437–441.

Goldberg, M. W., and T. D. Allen. 1992. High resolution scanning electron microscopy of the nuclear envelope: demonstration of a new, regular, fibrous lattice attached to the baskets of the nucleoplasmic face of the nuclear pores. *J. Cell Biol.* 119:1429–1440.

Green, M. R. 1991. Biochemical mechanisms of constitutive and regulated pre-mRNA splicing. *Annu. Rev. Cell Biol.* 7:559–599.

Hamm, J., and I. W. Mattaj. 1990. Monomethylated cap structures facilitate RNA export from the nucleus. *Cell.* 63:109–118.

He, D., J. A. Nickerson, and S. Penman. 1990. Core filaments of the nuclear matrix. *J. Cell Biol.* 110:569–580.

Herman, R. C., J. G. Williams, and S. Penman. 1976. Message and non-message sequences adjacent to poly(A) in steady state heterogeneous nuclear RNA of HeLa cells. *Cell.* 7:429–437.

Hinshaw, J. E., B. O. Carragher, and R. A. Milligan. 1992. Architecture and design of the nuclear pore complex. *Cell.* 69:1133–1141.

Hogan, N. C., K. L. Traverse, D. E. Sullivan, and M.-L. Pardue. 1994. The nucleus-limited Hsr-omega-n transcript is a polyadenylated RNA with a regulated intranuclear turnover. *J. Cell. Biol.* 125:21–30.

Huang, S., and D. L. Spector. 1991. Nascent pre-mRNA transcripts are associated with nuclear regions enriched in splicing factors. *Genes Dev.* 5:2288–2302.

Huang, S., and D. L. Spector. 1992. U1 and U2 small nuclear RNAs are present in nuclear speckles. *Proc. Natl. Acad. Sci. USA.* 89:305–308.

Ingles, E. J., A. Guialis, J. Lam, and L. Siminovitch. 1976. α-amanitin resistance of RNA polymerase II in mutant Chinese hamster ovary cell lines. *J.*

Biol. Chem. 251:2729–2734.
Jackson, D. A., A. B. Hassan, R. J. Errington, and P. R. Cook. 1993. Visualization of focal sites of transcription within human nuclei. *EMBO (Eur. Mol. Biol. Organ.) J.* 12:1059–1065.
Jacob, S. T., W. Muecke, E. M. Sajdel, and H. N. Munro. 1970. Evidence for extranucleolar control of RNA synthesis in the nucleolus. *Biochem. Biophys. Res. Commun.* 40:334–342.
Jarnik, M., and U. Aebi. 1991. Toward a more complete 3-D structure of the nuclear pore complex. *J. Struct. Biol.* 107:291–308.
Jiménez-García, L. F., and D. L. Spector. 1993. In vivo evidence that transcription and splicing are coordinated by a recruiting mechanism. *Cell.* 73:47–59.
Kedinger, C., J. L. Gniazdowski, J. L. Mandel Jr., F. Gissinger, and P. Chambon. 1970. α-amanitin: a specific inhibitor of one of two DNA-dependent RNA polymerase activities from calf thymus. *Biochem. Biophys. Res. Commun.* 38:165–171.
Kramerov, D. A., S. V. Tillib, G. P. Shumyatsky, and G. P. Georgiev. 1990. The most abundant nascent poly(A)$^+$ RNAs are transcribed by RNA polymerase III in murine tumor cells. *Nucleic Acids Res.* 18:4499–5506.
Lamond, A. I., and M. Carmo-Fonseca. 1993. The coiled body. *Trends Cell Biol.* 3:198–204.
Lindell, T. J., F. Weinberg, P. W. Morries, R. G. Roeder, and W.J. Rutter. 1970. Specific inhibition of nuclear RNA polymerase II by α-amanitin. *Science (Wash. DC).* 170:447–449.
Long, B. H., and W. H. Schrier. 1983. Isolation from Friend erythroleukemia cells of an RNase-sensitive nuclear matrix fibril fraction containing hnRNA and snRNA. *Biol. Cell.* 48:99–108.
Mariman, E., C. van Eekelen, R. Reinders, A. Berns, and W. van Venrooij. 1982. Adenoviral heterogeneous nuclear RNA is associated with the host nuclear matrix during splicing. *J. Mol. Biol.* 154:103–119.
Martin, T. E., S. C. Barghusen, G. P. Leser, and P.G. Spear. 1987. Redistribution of nuclear ribonucleoprotein antigens during Herpes simplex virus infection. *J. Cell Biol.* 105:2069–2082.
Mehlin, H., U. Skoglund, and B. Daneholt. 1991. Transport of Balbiani ring granules through nuclear pores in *Chironomus tentans*. *Exp. Cell Res.* 193:72–77.
Mehlin, H., B. Daneholt, and U. Skoglund. 1992. Translocation of a specific premessenger ribonucleoprotein particle through the nuclear pore studied with electron microscope tomography. *Cell.* 69:605–613.
Moore, J. M., C. C. Query, and P. A. Sharp. 1993. Splicing of precursors to mRNA by the spliceosome. *In* The RNA World. R. F. Gesteland and J. F. Atkins, editors. Cold Spring Harbor Laboratory Press, Cold Spring Harbor, NY. 303–357.
O'Keefe, R.T., A. Mayeda, C. L. Sadowski, A. R. Krainer, and D. L. Spector. 1994. Disruption of pre-mRNA splicing in vivo results in reorganization of splicing factors. *J. Cell Biol.* 246–260.
Penman, S., M. Rosbash, and M. Penman. 1970. Messenger and heterogeneous nuclear RNA in HeLa cells: differential inhibition by cordycepin. *Proc. Natl. Acad. Sci. USA.* 67:1878–1885.
Perry, R.P., D. E. Kelley, and J. LaTorre. 1974. Synthesis and turnover of nuclear and cytoplasmic polyadenylic acid in mouse L cells. *J. Mol. Biol.* 82:315–331.
Phelan, A., M. Carmo-Fonseca, J. McLauchlan, A. I. Lamond, and J. B. Clements. 1993. A Herpes simplex virus type 1 immediate-early gene product, IE63, regulates small nuclear ribonucleoprotein distribution. *Proc. Natl. Acad. Sci. USA.* 90:9056–9060.
Puvion, E., and W. Bernhard. 1975. Ribonucleoprotein components in liver cell nuclei as visualized by cryoultramicrotomy. *J. Cell Biol.* 67:200–214.
Ramon y Cajal, S. 1903. Un sencillo metodo de coloracion selectiva del reticulo protoplasmico y sus efectos en los diversos organos nerviosos. *Trab. Lab. Invest. Biol.* 2:129–221.
Raska, I., L. E. C. Andrade, R. L. Ochs, E. K. L. Chan, C.-M. Chang, G. Roos, and E. M. Tan. 1991. Immunological and ultrastructural studies of the nuclear coiled body with autoimmune antibodies. *Exp. Cell Res.* 195:27–37.
Reed, R. 1990. Protein composition of mammalian spliceosomes assembled *in vitro*. *Proc. Natl. Acad. Sci. USA.* 87:8031–8035.
Ris, H. 1989. Three-dimensional imaging of cell ultrastructure with high resolution low voltage SEM. *Inst. Phys. Conf. Ser.* 98:657–662.
Ris, H. 1991. The three-dimensional structure of the nuclear pore complex as seen by high voltage electron microscopy and high resolution low voltage scanning electron microscopy. *EMSA Bull.* 21:54–56.
Schindler, M., and L.-W. Jiang. 1986. Nuclear actin and myosin as control elements in nucleocytoplasmic transport. *J. Cell Biol.* 102:859–862.
Schroder, H. C., U. Friese, M. Bachmann, T. Zaubitzer, and W. E. G. Muller. 1989. Energy requirement and kinetics of transport of poly A-free histone mRNA compared to poly A-rich mRNA from isolated L-cell nuclei. *Eur. J. Biochem.* 181:149–158.
Smetana, K., W. J. Steele, and H. Busch. 1963. A nuclear ribonucleoprotein network. *Exp. Cell Res.* 31:198–201.
Smith, H. C., R. L. Ochs, E. A. Fernandez, and D. L. Spector. 1986. Macromolecular domains containing nuclear protein p107 and U-snRNP protein p28: further evidence for an *in situ* nuclear matrix. *Mol. Cell. Biochem.* 70:151–168.
Spector, D. L. 1990. Higher order nuclear organization: three-dimensional distribution of small nuclear ribonucleoprotein particles. *Proc. Natl. Acad. Sci. USA.* 87:147–151.
Spector, D. L. 1993. Macromolecular domains within the cell nucleus. *Annu. Rev. Cell Biol.* 9:265–315.
Spector, D. L., W. H. Schrier, and H. Busch. 1983. Immunoelectron microscopic localization of snRNPs. *Biol. Cell.* 49:1-10.
Spector, D. L., X.-D. Fu, and T. Maniatis. 1991. Associations between distinct pre-mRNA splicing components and the cell nucleus. *EMBO (Eur. Mol. Biol. Organ.) J.* 10:3467–3481.
Spector, D. L., G. Lark, and S. Huang. 1992. Differences in snRNP localization between transformed and nontransformed cells. *Mol. Biol. Cell.* 3:555–569.
Spector, D. L., R. T. O'Keefe, and L. F. Jiménez-García. 1993. Dynamics of transcription and pre-mRNA splicing within the mammalian cell nucleus. *Cold Spring Harbor. Symp. Quant. Biol.* 58:799–805.
Stirpe, F., and L. Fiume. 1967. Studies on the pathogenesis of liver necrosis by α-amanitin. Effect of α-amanitin on ribonucleic acid synthesis and on ribonucleic acid polymerase in mouse liver nuclei. *Biochem. J.* 105:779–782.
Tamm, I., and P. B. Sehgal. 1978. Halobenzimidazole ribosides and RNA synthesis of cells and viruses. *Adv. Virus Res.* 22:187–258.
Thiry, M. 1993. Differential location of nucleic acids within interchromatin granule clusters. *Eur. J. Cell Biol.* 62:259–269.
Turner, B. M., and L. Franchi. 1987. Identification of protein antigens associated with the nuclear matrix and with clusters of interchromatin granules in both interphase and mitotic cells. *J. Cell Sci.* 87:269–282.
van Eekelen, C. A. G., and W. J. van Venrooij. 1981. hnRNA and its attachment to a nuclear protein matrix. *J. Cell Sci.* 88:554–563.
Visa, N., F. Puvion-Dutilleul, F. Harper, J.-P. Bachellerie, and E. Puvion. 1993. Intranuclear distribution of poly A RNA determined by electron microscope in situ hybridization. *Exp. Cell. Res.* 208:19–34.
Vogelstein, B., and B. F. Hunt. 1982. A subset of small nuclear ribonucleoprotein particle antigens is a component of the nuclear matrix. *Biochem. Biophys. Res. Commun.* 105:1224–1232.
Wansink, D. G., W. Schul, I. van der Kraan, B. van Steensel, R. van Driel, and L. de Jong. 1993. Fluorescent labeling of nascent RNA reveals transcription by RNA polymerase II in domains scattered throughout the nucleus. *J. Cell Biol.* 122:283–293.
Weinmann R., and R. G. Roeder. 1974. Role of DNA-dependent RNA polymerase III in the transcription of the tRNA and 5S RNA genes. *Proc. Natl. Acad. Sci. USA.* 71:1790–1794.
Xing, Y., and J. B. Lawrence. 1991. Preservation of specific RNA distribution within the chromatin-depleted nuclear substructure demonstrated by in situ hybridization coupled with biochemical fractionation. *J. Cell Biol.* 112: 1055–1063.
Xing, Y., C. V. Johnson, P. R. Dobner, and J. B. Lawrence. 1993. Higher level organization of individual gene transcription and RNA splicing. *Science (Wash. DC).* 259:1326–1330.
Zachar, Z., J. Kramer, and P. M. Bingham. 1993. Evidence for channeled diffusion of pre-mRNAs during nuclear RNA transport in metazoans. *J. Cell Biol.* 121:729–742.
Zeitlin, S., A. Parent, S. Silverstein, and A. Efstratiadis. 1987. Pre-mRNA splicing and the nuclear matrix. *Mol. Cell. Biol.* 7:111–120.
Zeitlin, S., R. C. Wilson, and A. Efstratiadis. 1989. Autonomous splicing and complementation of in vivo-assembled spliceosomes. *J. Cell Biol.* 108: 765–777.
Zeng, C., D. He, S. Berget, and B. R. Brinkley. 1994. NuMA: A structural protein interface between the nucleoskeleton and RNA splicing. *Proc. Natl. Acad. Sci. USA.* 91:1505–1509.